Selected Topics in Advanced Optics

Week 6 – part 1

Olivier J.F. Martin
Nanophotonics and Metrology Laboratory

EPFL

Optics of metals and plasmonics
Part II – Propagating plasmons

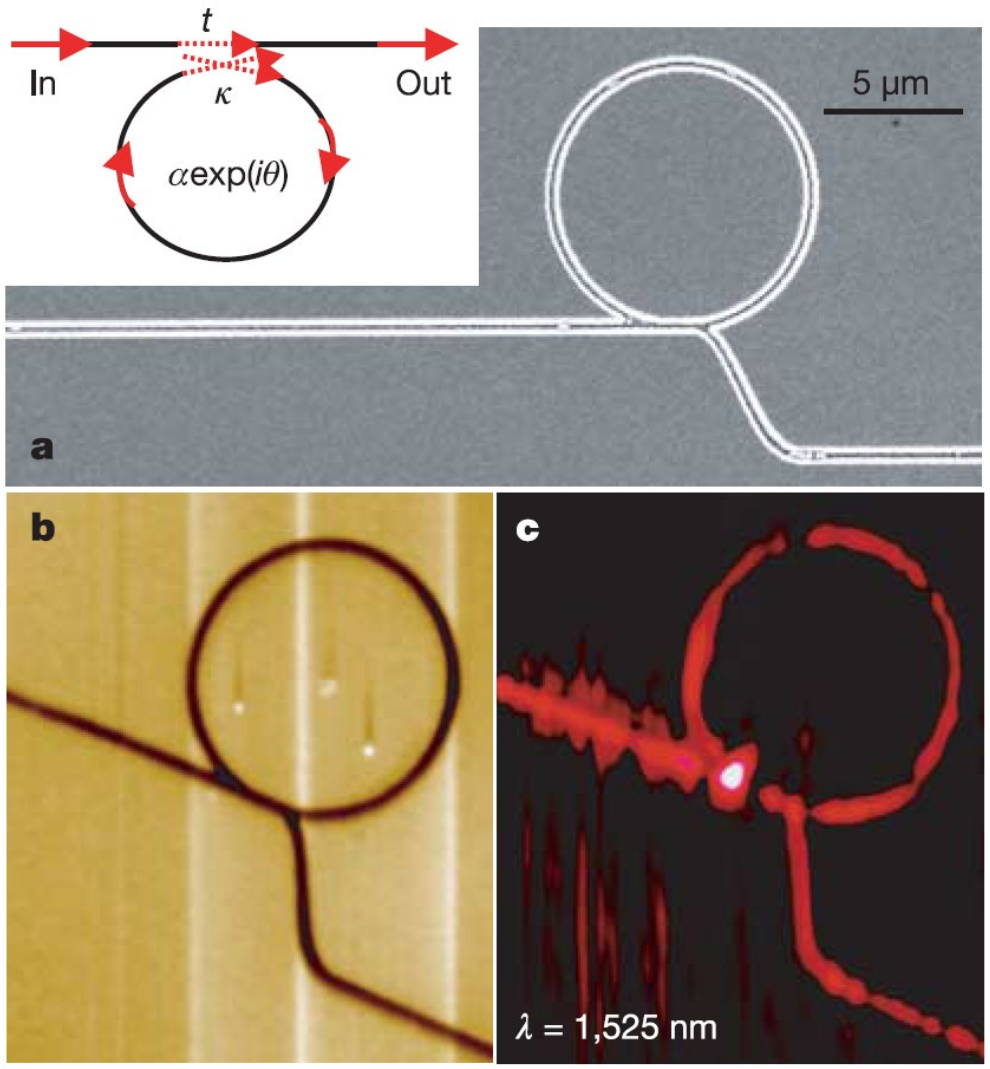

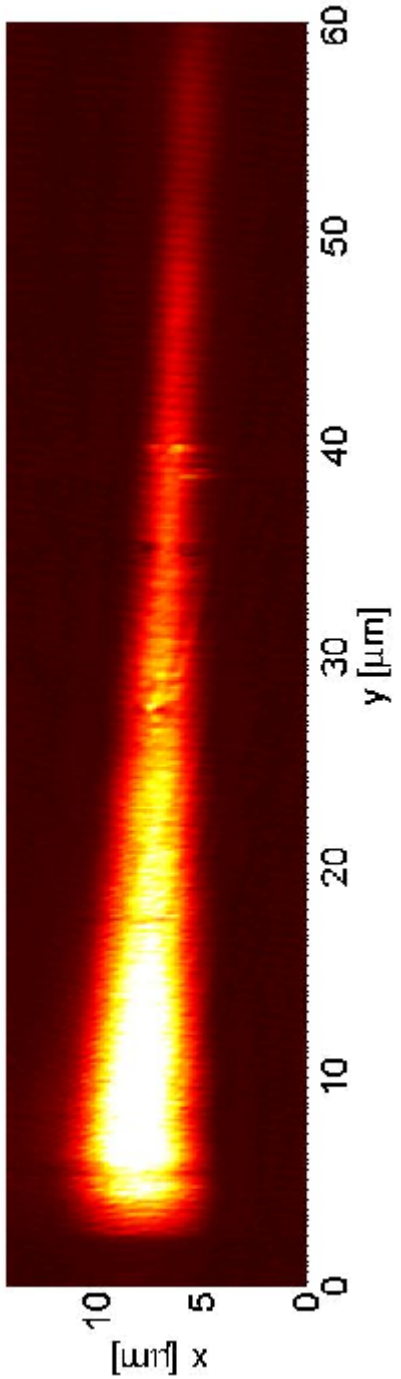

Some references

- H. Raether, Surface Plasmons on Smooth and Rough Surfaces and on Gratings, Springer Tracts in Modern Physics **111** (Springer, New York, 1988).
- S.A. Maier, Plasmonics: Fundamentals and Applications (Springer, 2007).
- J. Homola, Surface plasmon resonance based sensors, SpringerSeries in Chemical Sensors and Biosensors **4** (Springer, Berlin, 2006).
- P. Berini, “Long-range surface plasmon polaritons”, *Adv. in Opt. and Photon.* **1**, 484-588 (2009).
- M.L. Brongersma and P.G. Kik (Eds.), Surface plasmon nanophotonics (Springer, 2007).

SPP dispersion relation on a semi-infinite metal (Raether)

p-polarized wave:

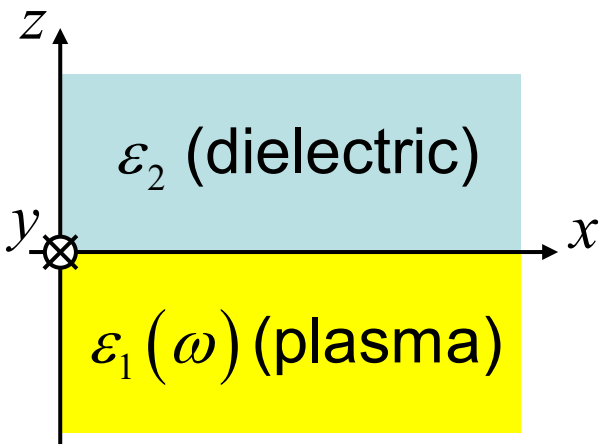

$$\begin{cases} \mathbf{E}_2 = (E_{2x}, 0, E_{2z}) \exp i(k_{2x}x + k_{2z}z - \omega t) \\ \mathbf{H}_2 = (0, H_{2y}, 0) \exp i(k_{2x}x + k_{2z}z - \omega t) \end{cases}$$

$$\begin{cases} \mathbf{E}_1 = (E_{1x}, 0, E_{1z}) \exp i(k_{1x}x - k_{1z}z - \omega t) \\ \mathbf{H}_1 = (0, H_{1y}, 0) \exp i(k_{1x}x - k_{1z}z - \omega t) \end{cases}$$

Maxwell's equations :

(1) $\nabla \times \mathbf{E}_i = i\omega\mu_0 \mathbf{H}_i$

(2) $\nabla \times \mathbf{H}_i = -i\omega\varepsilon_0\varepsilon_i \mathbf{E}_i$

(3) $\varepsilon_0\varepsilon_i \nabla \cdot \mathbf{E}_i = 0$

(4) $\nabla \cdot \mathbf{H} = 0$

Continuity at the interface :

$E_{1x} = E_{2x}$ (5a)

$H_{1y} = H_{2y}$ (5b)

$\varepsilon_1 E_{1z} = \varepsilon_2 E_{2z}$

$k_{1x} = k_{2x} = k_x$

SPP dispersion relation on a semi-infinite metal

$$(2)\ \text{leads to}: \frac{\partial H_{iy}}{\partial z} = i\omega\varepsilon_0\varepsilon_i E_{ix} \qquad \begin{aligned} k_{1z}H_{1y} &= -\omega\varepsilon_0\varepsilon_1 E_{1x} \\ k_{2z}H_{2y} &= \omega\varepsilon_0\varepsilon_2 E_{2x} \end{aligned}$$

$$\text{using}\ (5): \begin{cases} H_{1y} - H_{2y} = 0 \\ \dfrac{k_{1z}}{\varepsilon_1}H_{1y} + \dfrac{k_{2z}}{\varepsilon_2}H_{2y} = 0 \end{cases}$$

$$\text{solution if } \det = 0: \det = \frac{k_{2z}}{\varepsilon_2} + \frac{k_{1z}}{\varepsilon_1}$$

$$\text{furthermore}: k_x^2 + k_{iz}^2 = \varepsilon_i \frac{\omega^2}{c^2}$$

$$\text{it follows}: \boxed{k_x = \frac{\omega}{c}\left(\frac{\varepsilon_1\varepsilon_2}{\varepsilon_1 + \varepsilon_2}\right)^{1/2}}$$

SPP dispersion relation on a semi-infinite metal

Metal with complex permittivity : $\varepsilon_1 = \varepsilon_1' + i\varepsilon_1''$

covered with dielectric : ε_2 real

Complex propagation vector : $k_x = k_x' + ik_x''$

$$k_x' = \frac{\omega}{c}\left(\frac{\varepsilon_1'\varepsilon_2}{\varepsilon_1' + \varepsilon_2}\right)^{1/2} \qquad k_x'' = \frac{\omega}{c}\left(\frac{\varepsilon_1'\varepsilon_2}{\varepsilon_1' + \varepsilon_2}\right)^{3/2} \frac{\varepsilon_1''}{2\left(\varepsilon_1'\right)^2}$$

SPP dispersion relation on a semi-infinite Drude metal in air

Drude metal : $\varepsilon_1(\omega) = 1 - \dfrac{\omega_p^2}{\omega(\omega + i\gamma)}$

$$k_x' = \frac{\omega}{c}\left(\frac{\omega^2 - \omega_p^2}{2\omega^2 - \omega_p^2}\right)^{1/2} \qquad (\omega \gg \gamma)$$

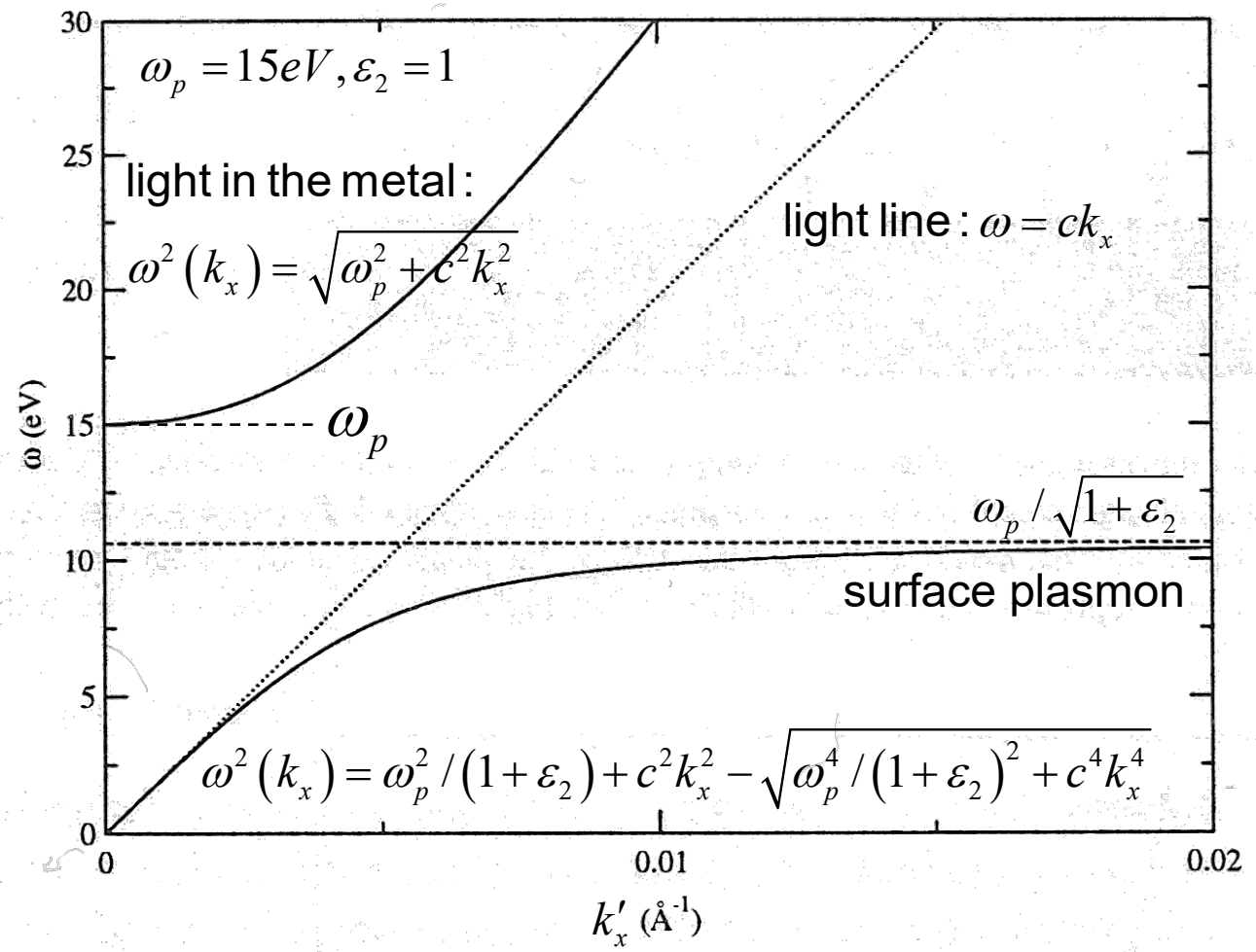

Localized and propagating plasmons for a Drude metal

$$\varepsilon_1(\omega) = 1 - \frac{\omega_p^2}{\omega(\omega + i\gamma)}$$

- The propagating or SPP mode is a dispersive mode: the frequency ω and the momentum k change continuously
- The localized plasmon resonance does not disperse: its frequency ω is constant, irrespective of the momentum k
- Propagating mode (SPP) :

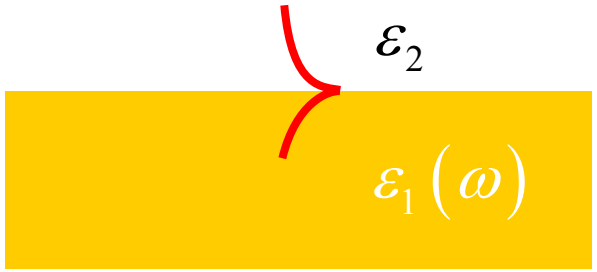

$$k_x' = \frac{\omega}{c}\left(\frac{\omega^2 - \omega_p^2}{2\omega^2 - \omega_p^2}\right)^{1/2}$$

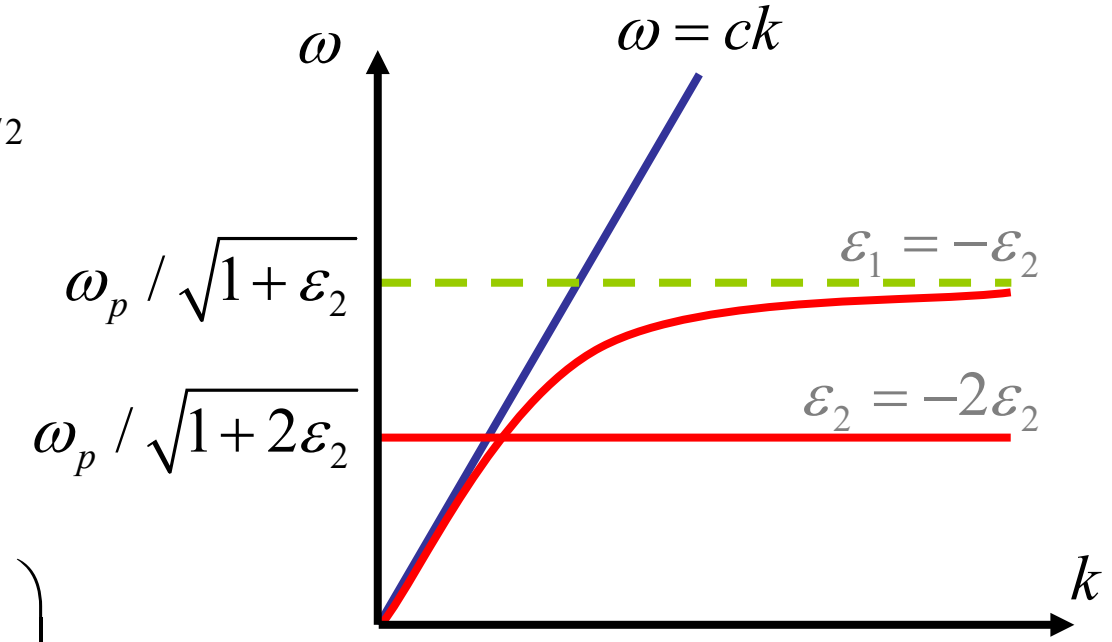

- Localized mode (LSPR):

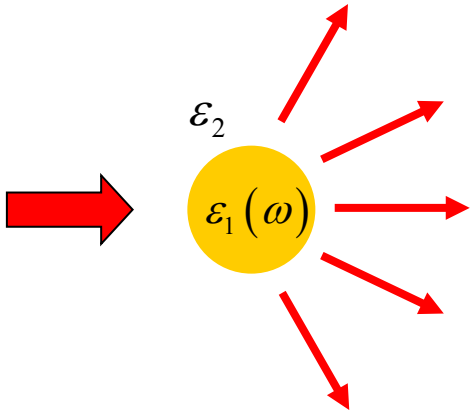

$$\alpha(\omega) \approx \left(\frac{\varepsilon_1(\omega) - \varepsilon_2}{\varepsilon_1(\omega) + 2\varepsilon_2}\right)$$

SPP dispersion relation on a semi-infinite metal

- There is localization of the charges along the metal surface
- The field distribution decays very rapidly away from the interface

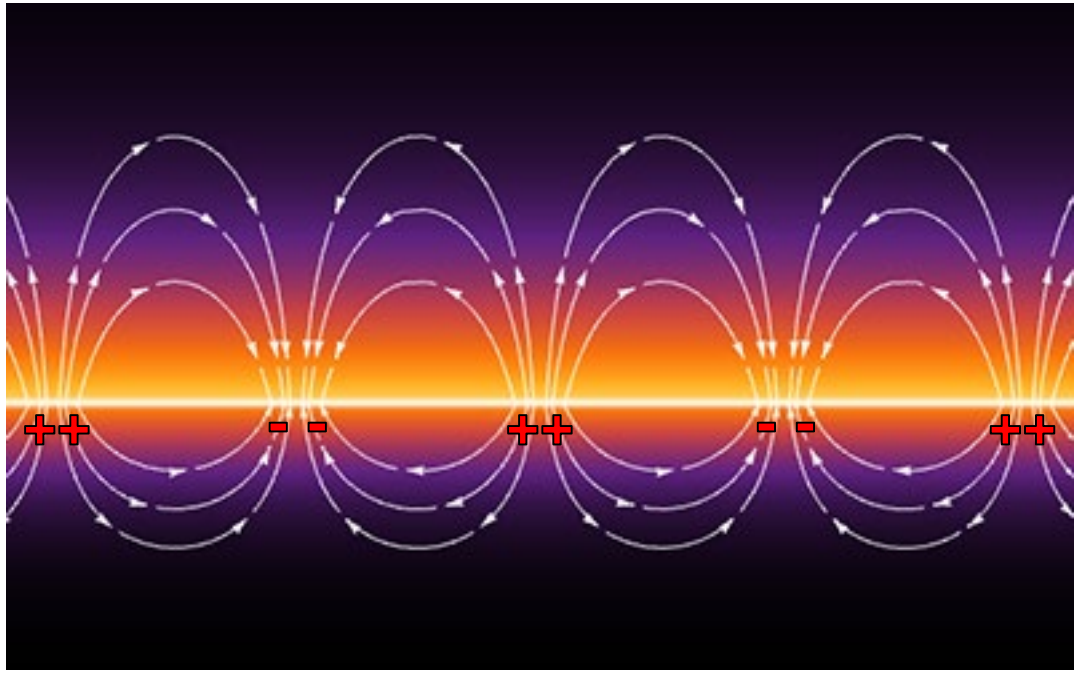

D.R. Smith, Duke University

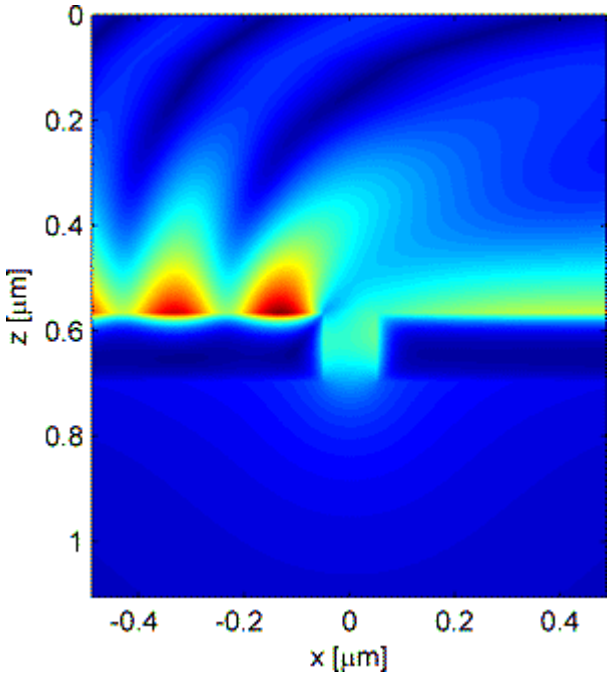

SPP coupling to a groove in a metallic film

Oulu University, Finland

SPP dispersion relation on a semi-infinite metal

- The dispersion relation changes with the dielectric function of the covering material on the top of the metal film

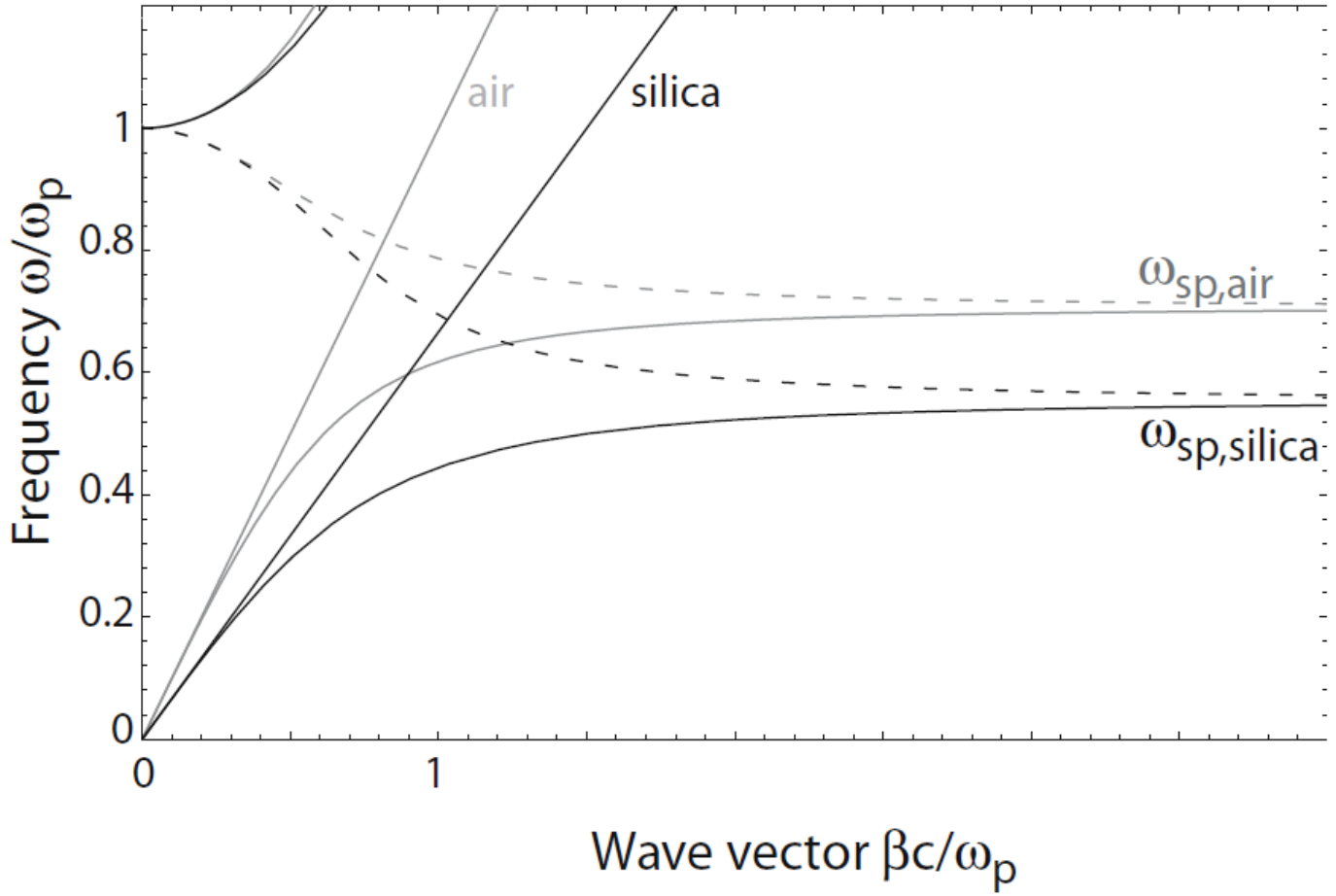

S.A. Maier, Plasmonics: Fundamentals and Applications (Springer, 2007).

Selected Topics in Advanced Optics

Week 6 – part 2

Olivier J.F. Martin
Nanophotonics and Metrology Laboratory

EPFL

SPP dispersion relation on a thin film

Derivation based on the reflectivity (p-polarized wave):

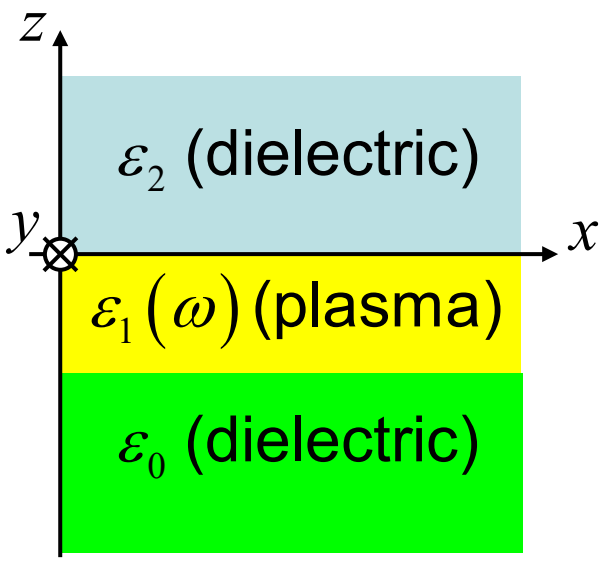

For each interface :

$$r_{ij} = \left(\frac{k_{iz}}{\varepsilon_i} - \frac{k_{jz}}{\varepsilon_j} \right) / \left(\frac{k_{iz}}{\varepsilon_i} + \frac{k_{jz}}{\varepsilon_j} \right) \qquad t_{ij} = 1 + r_{ij}$$

For the total system :

$$r_{012} = \frac{E_r}{E_0} = \frac{r_{01} + r_{12} \exp(2i\alpha)}{1 + r_{01} r_{12} \exp(2i\alpha)} \qquad \alpha = k_{1z} d$$

$$(2i\alpha < 0, \text{since } \varepsilon_1 < 0)$$

The zero of the denominator of r_{012} give the dispersion relation of the system:

$$1 + r_{01} r_{12} \exp(2i\alpha) = 0$$

SPP dispersion relation on a thin film – Intuitive approach

- Consider two surface plasmons on two interfaces:

- When the metal becomes thin, the two modes will couple:

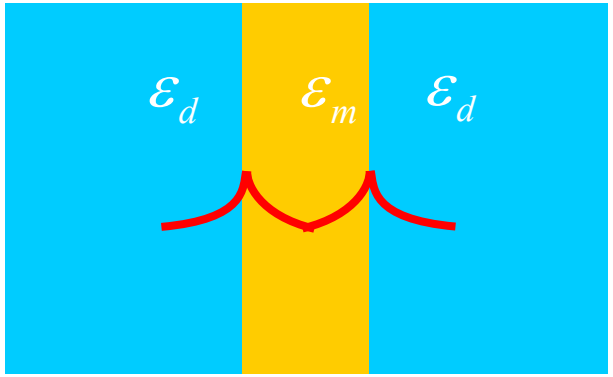

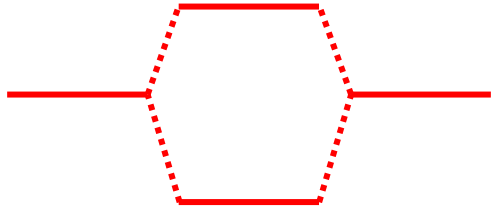

Hybridization model

- This will produce two different modes: a long-range and a short range mode

P. Berrini, Advances in Optics and Photonics vol. 1, p. 484 (2009)

Long-range and short-range SPP (propagation normal to the plane of the figure)

- Propagation along z
- The long-range mode has symmetric dominant electric field E_y
- The short-range mode has antisymmetric E_y
- Other components:
  - H_x same symmetry as E_y
  - E_z opposite symmetry as E_y

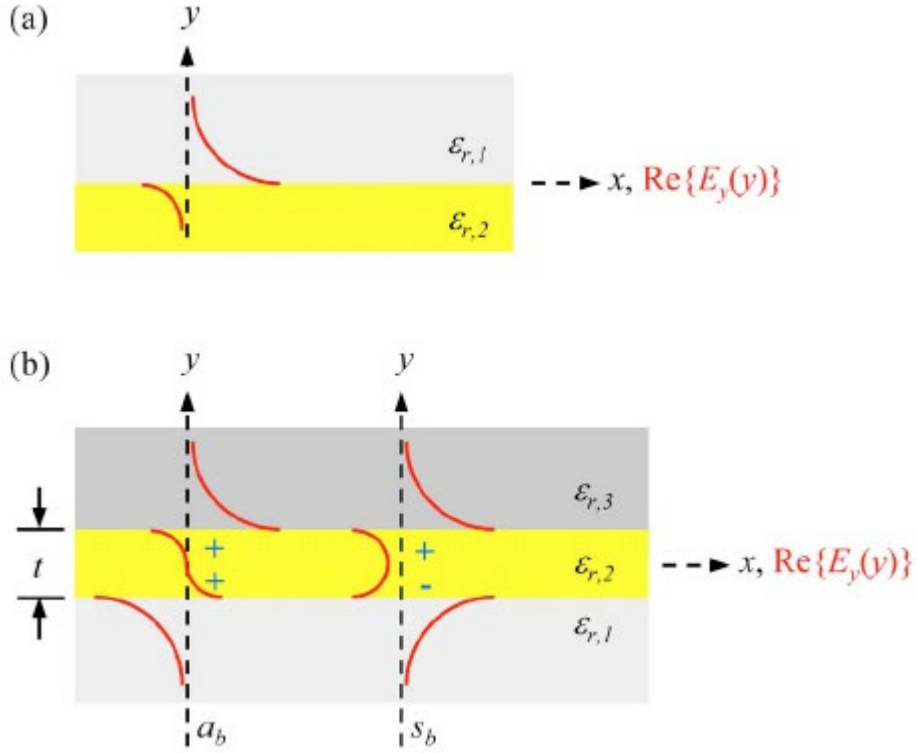

Table 1. Model Properties of SPP Waveguides

Mode, Structure	$n_{eff}-n_1$	MPA (dB/mm)	L_e (μm)	δ_w (μm)
SPP, single interface	0.013	44	98	1.27
LRSPP (S_b mode), metal slab	0.0023	1.2	3776	6.12

P. Berrini, Advances in Optics and Photonics vol. 1, p. 484 (2009)

Long-range vs. short range SPP (propagation in the plane of the figure)

- They have opposite charge distribution:

Short range

Long range

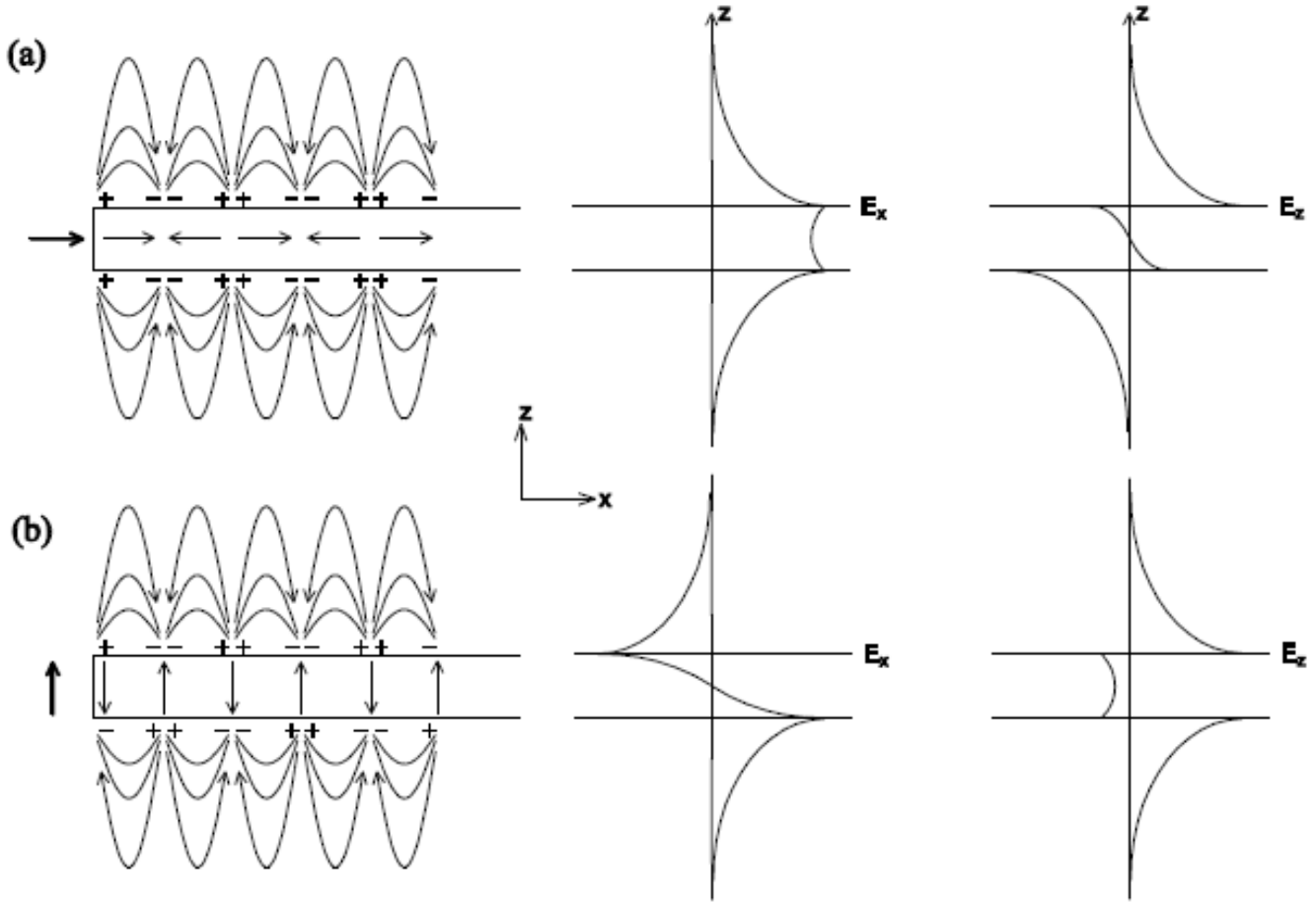

Fig. 3. Effect of horizontal and vertical dipole sources on an infinitely long metallic nanoparticle and the resulting electric field distributions. (a) A horizontal dipole excites the even propagating mode, while (b) a vertical dipole excites the odd mode.

Excitation of SPP

- Direct excitation is not possible (from air), k is too short !

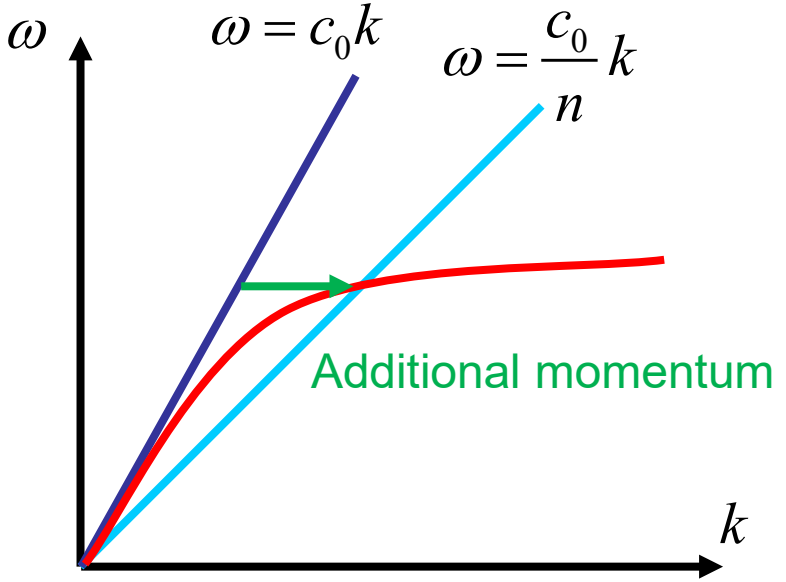

- There are different ways to provide additional momentum to match the SPP propagation vector:

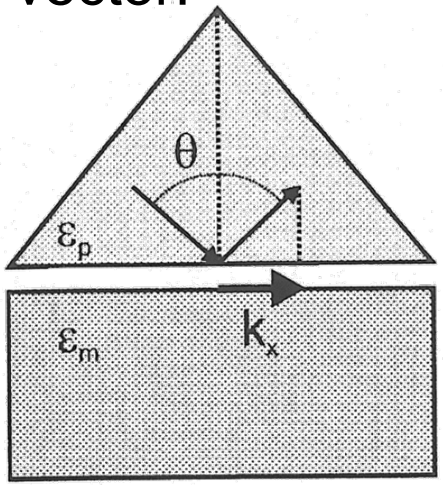

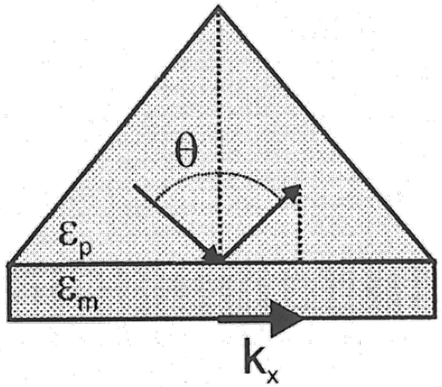

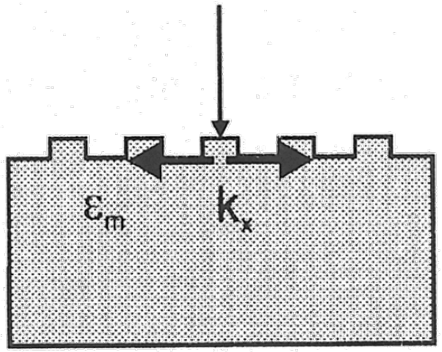

SPP excitation on a thin film

- Au film on a glass substrate, different thicknesses: when the SPP is excited, most of the incident energy goes into that mode and very little light is reflected

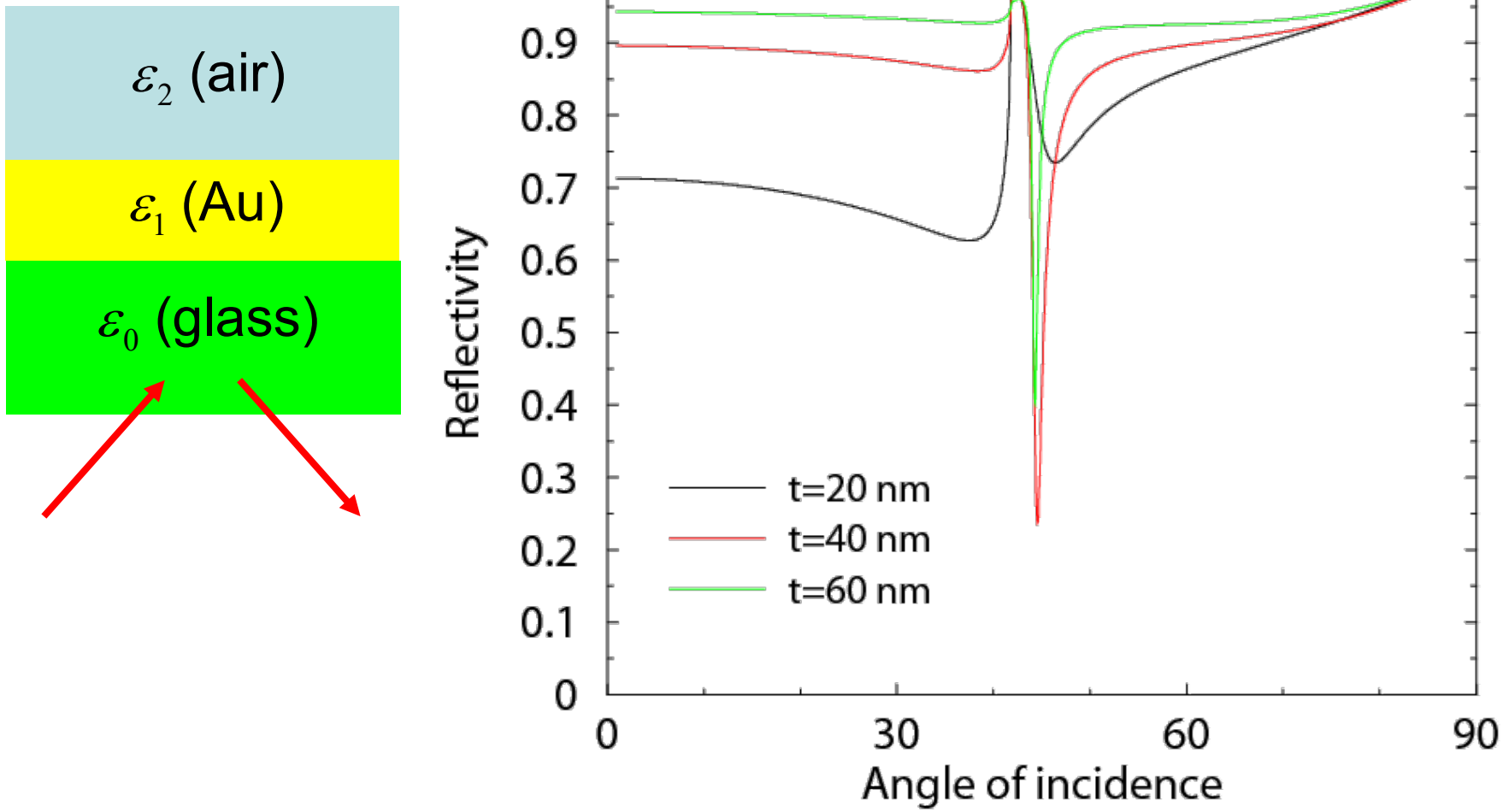

Selected Topics in Advanced Optics

Week 6 – part 3

Olivier J.F. Martin
Nanophotonics and Metrology Laboratory

EPFL

Direct SPP measurement using heterodyne photon scanning tunneling microscopy (PSTM)

- The SPP has a larger momentum k than a wave propagating in free space
- Its effective wavelength λ should be smaller $\left(\lambda = 2\pi / k\right)$

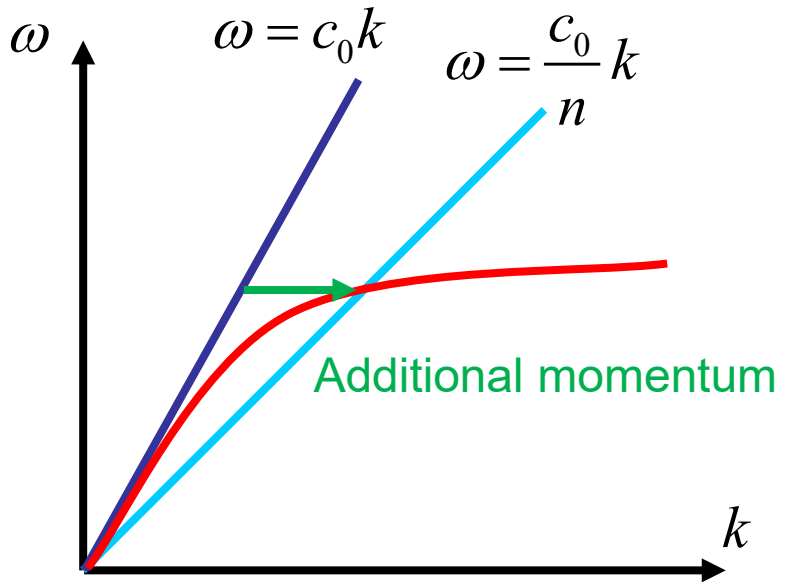

- Can we measure this experimentally?

Direct SPP measurement using heterodyne photon scanning tunneling microscopy (PSTM)

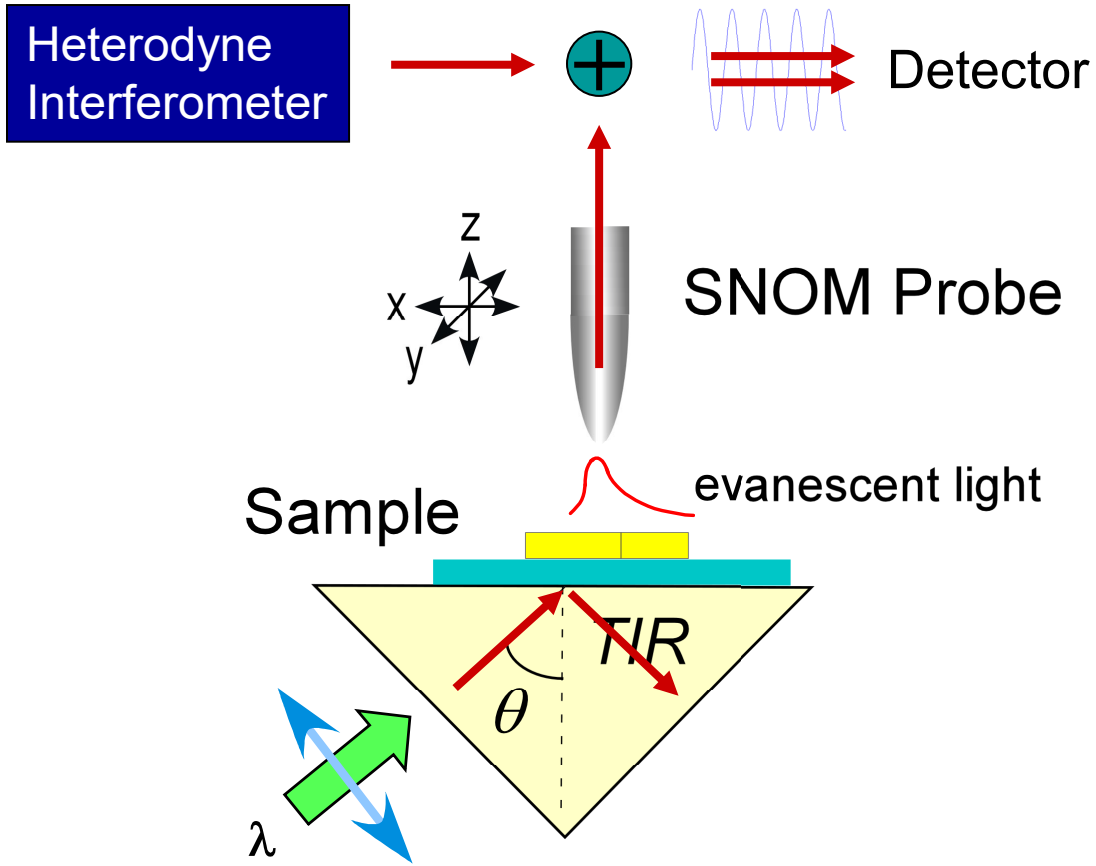

- Shear force AFM:

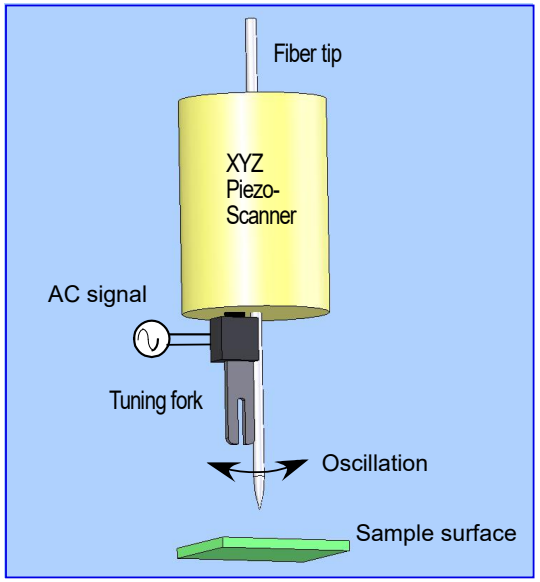

resolution: x,y ~ 1 nm
z ~ 5 nm

- Coherent PSTM combined with heterodyne interferometer
  → measurement of the amplitude and phase of the field !

Heterodyne photon scanning tunneling microscopy (PSTM)

- In addition to the phase measurement, this interferometric technique provides very high sensitivity (shot-noise limited)

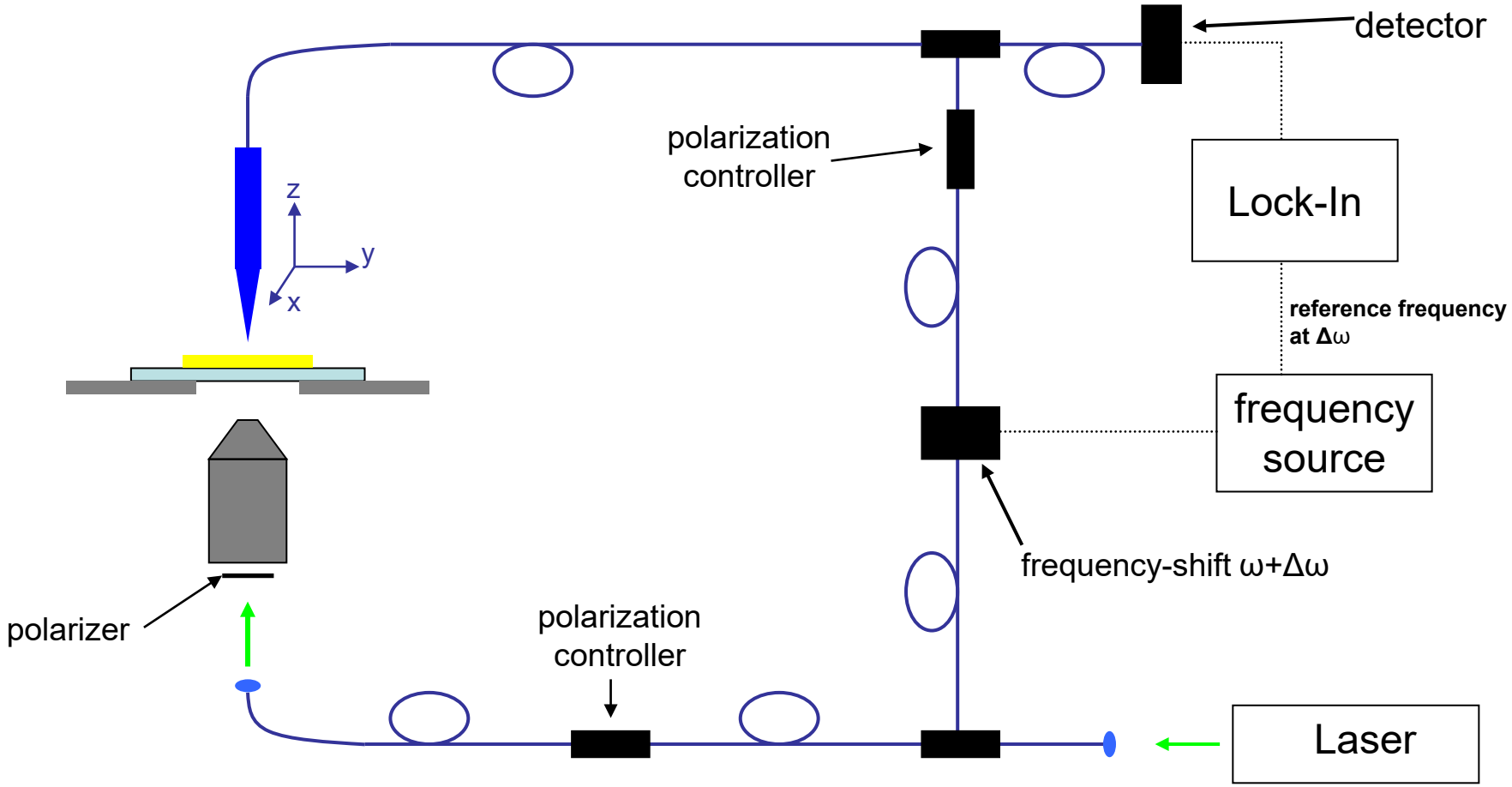

Heterodyne photon scanning tunneling microscopy (PSTM)

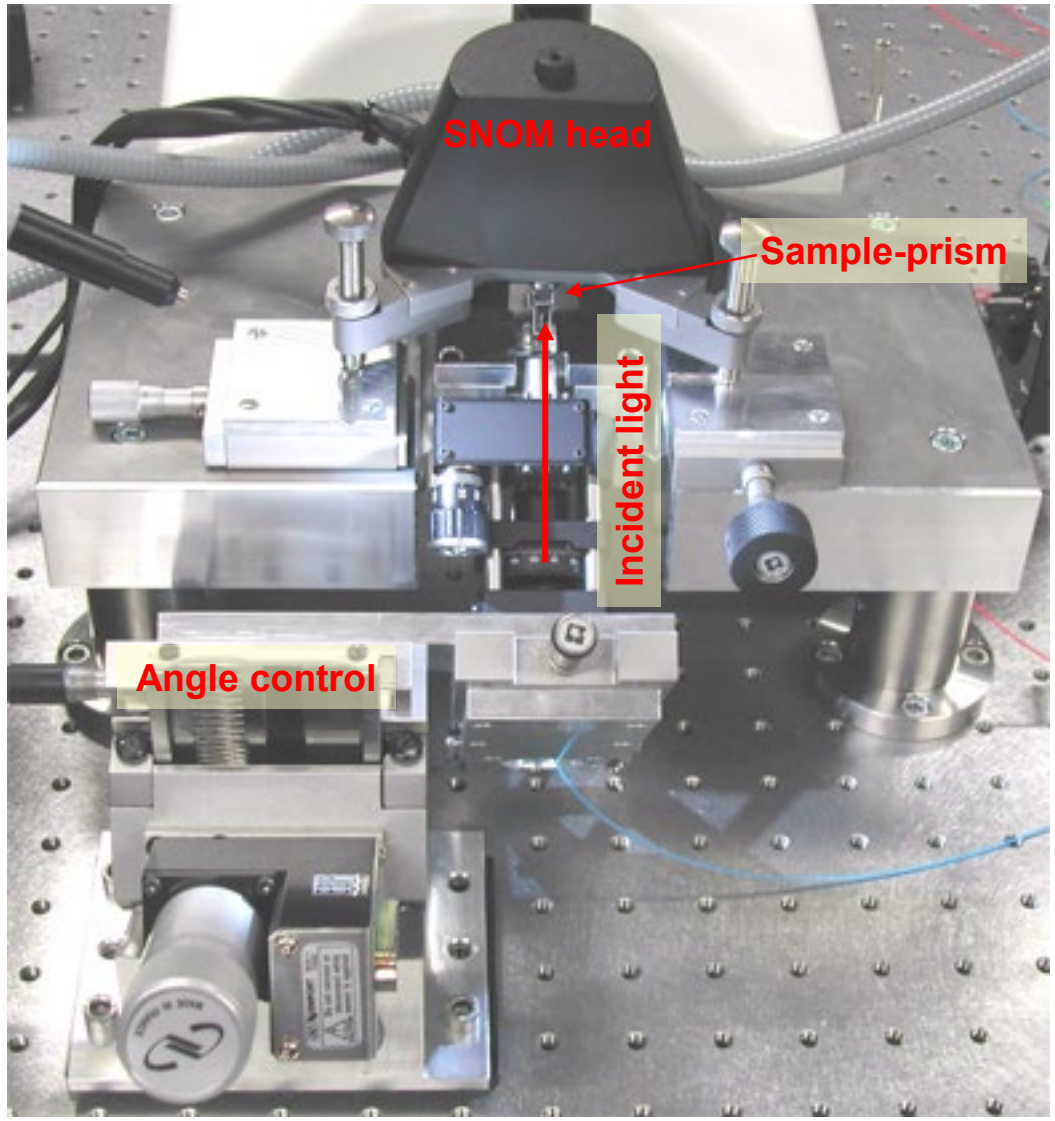

Tuning fork

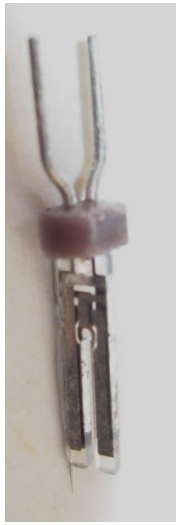

Fiber probe (ρ ~ 50 nm)

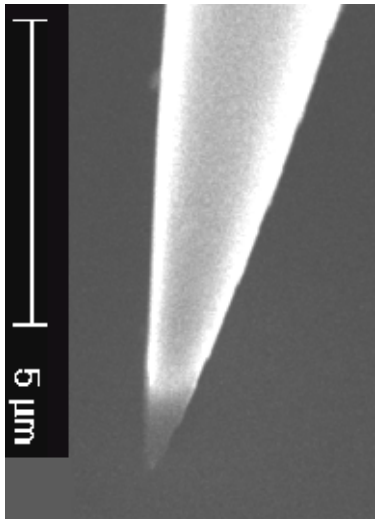

Gold waveguide topography

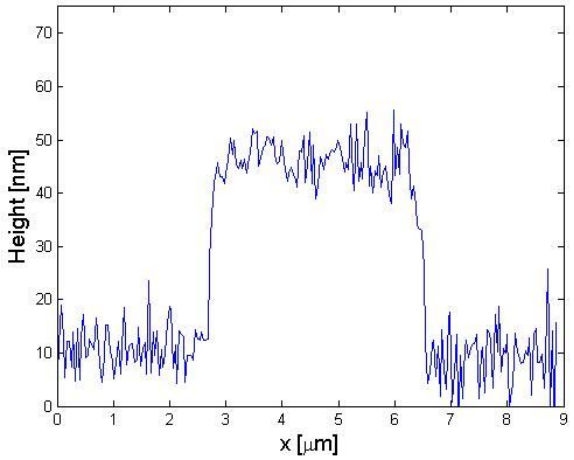

Direct SPP measurement using heterodyne photon scanning tunneling microscopy (PSTM)

λ_0 = 690 nm

Amplitude

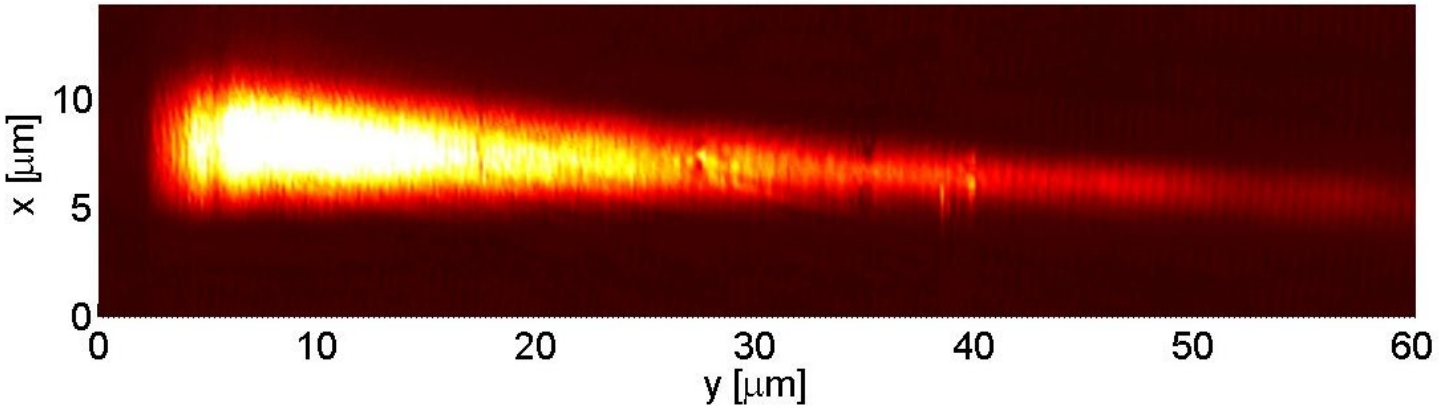

Phase

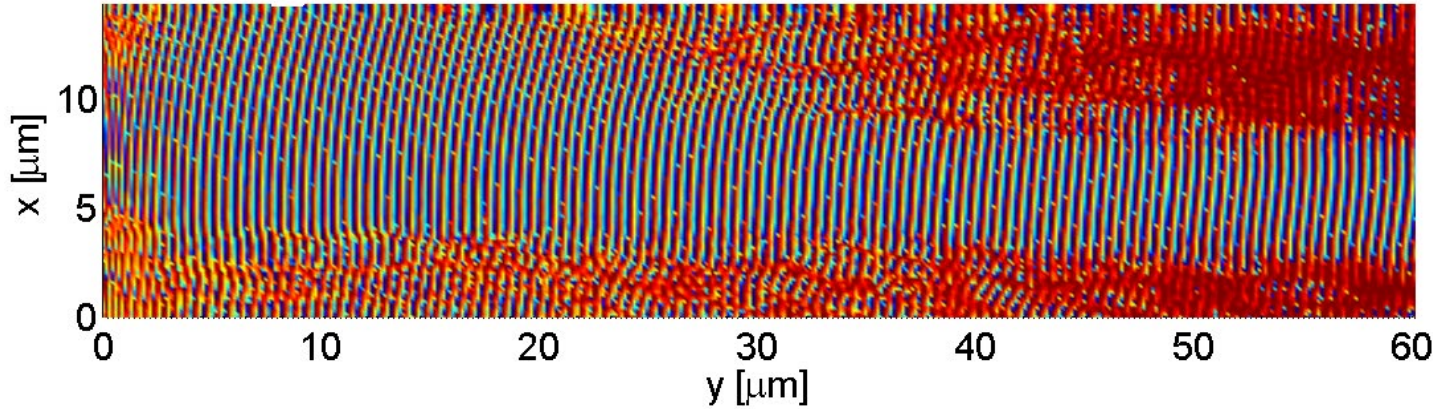

Direct SPP measurement using heterodyne photon scanning tunneling microscopy (PSTM)

Amplitude

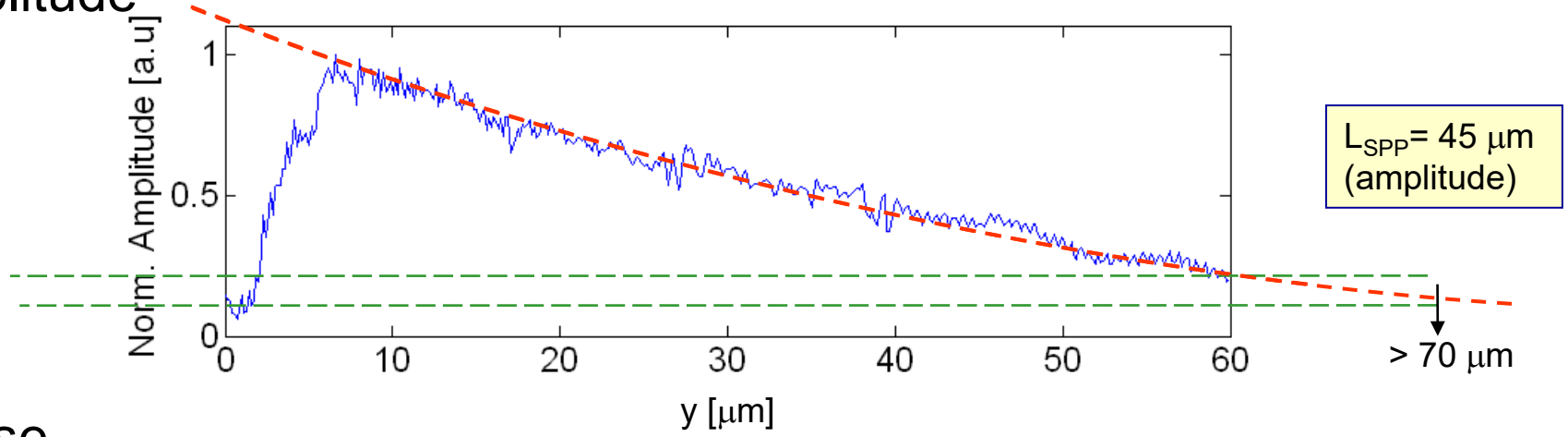

L_{SPP}= 45 μm (amplitude)

Phase

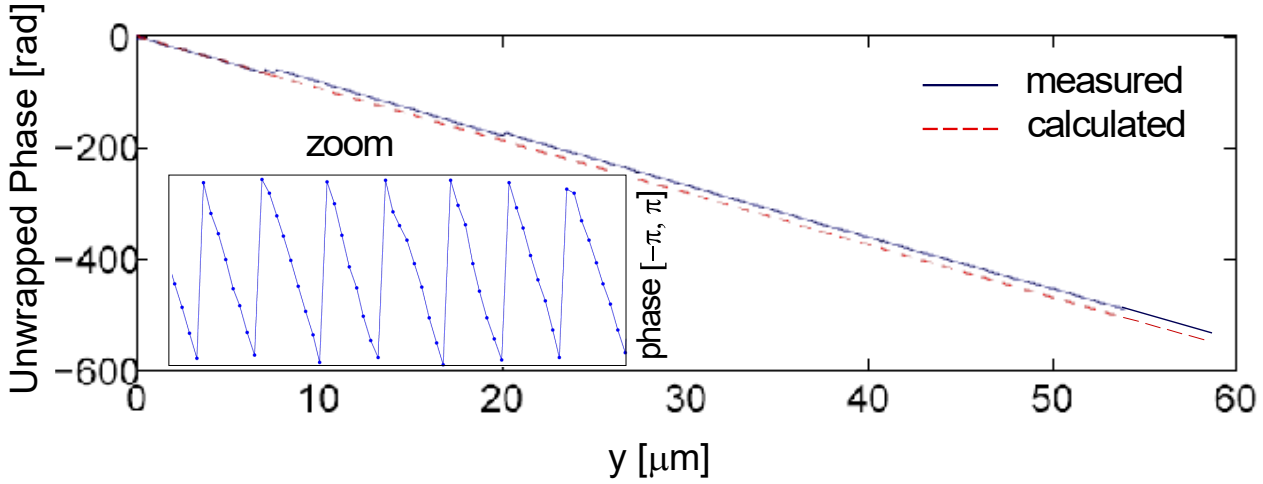

$$\lambda_{SPP} = \frac{1}{2\pi}\left(-\Delta\phi/\delta y\right)^{-1} = 670\,nm$$

- The illumination wavelength was λ_0=690 nm, hence the effective wavelength is smaller, which is a characteristics of a surface wave!

SPP reflection/refraction

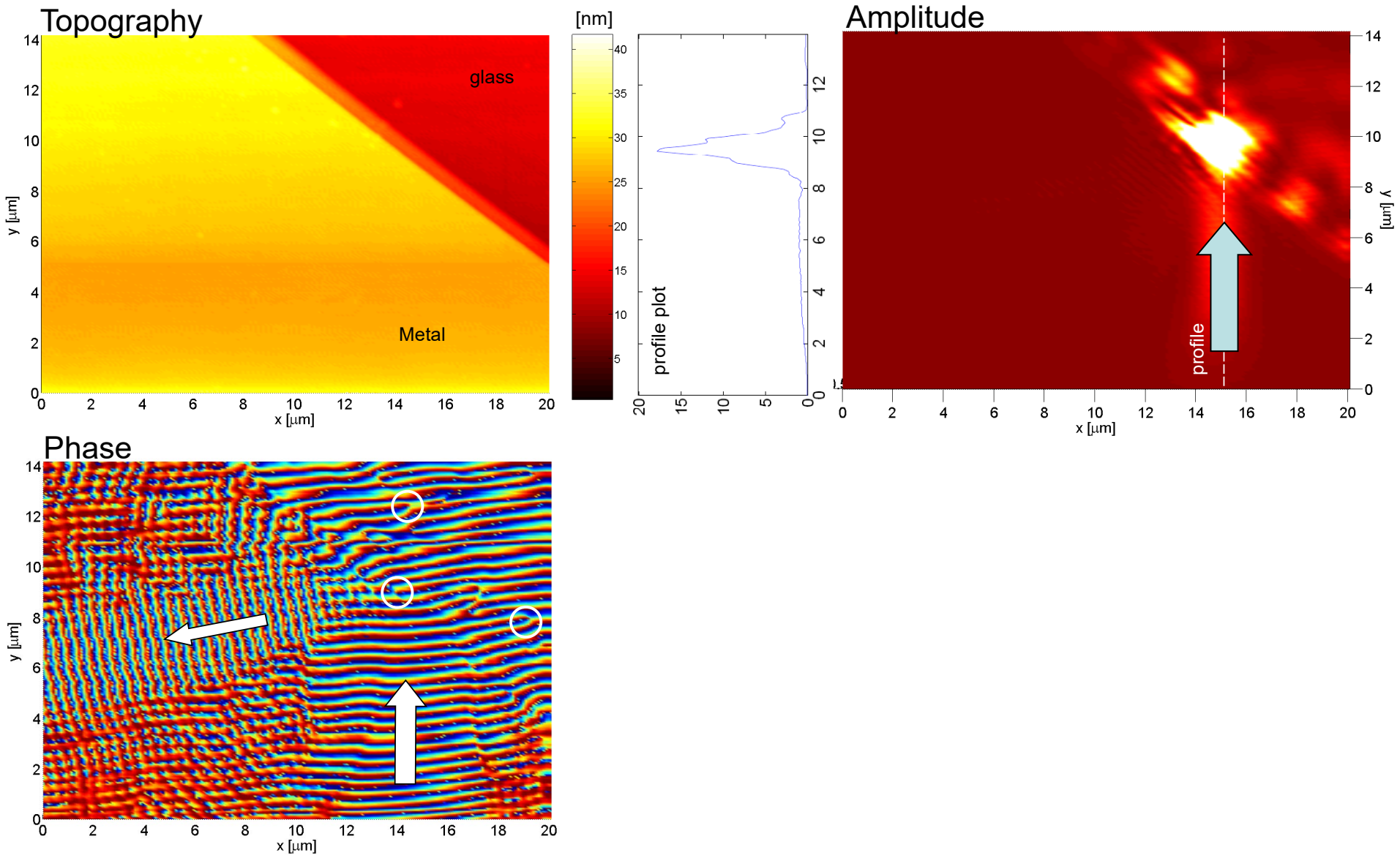

Olivier J.F. Martin

Link with localized plasmon resonance

- If one takes a metal particle and stretches it, one should slowly reach the condition for a propagating plasmon

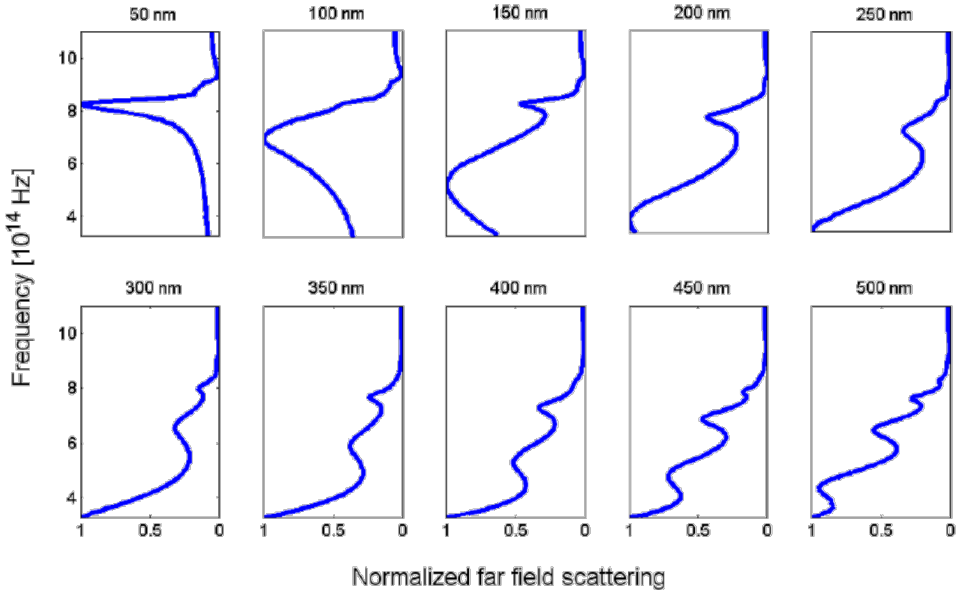

Fig. 6. Normalized scattering spectra for particles of L = 50-500nm, excited by a θ = 0° dipole source. For successively larger lengths L, higher order modes are excited.

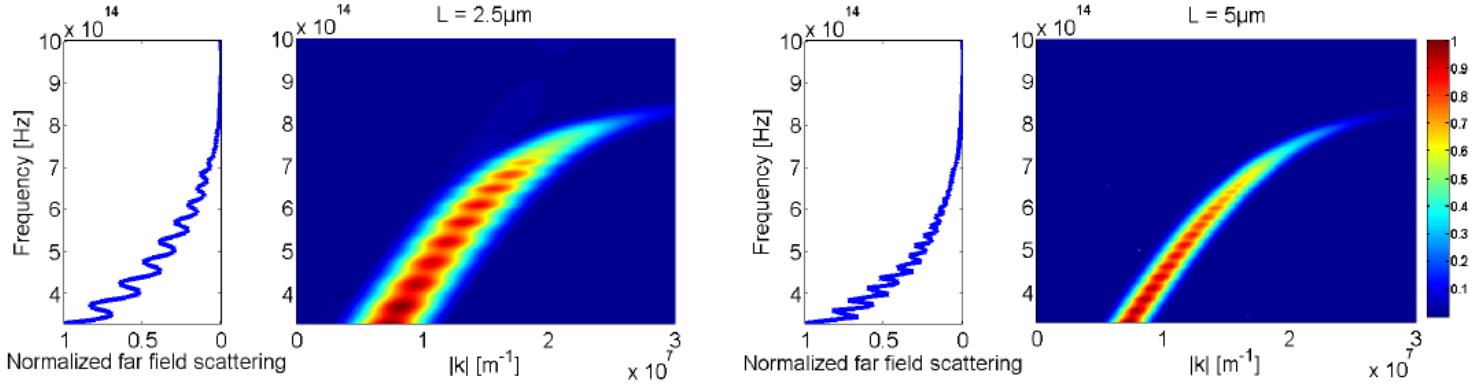

Fig. 7. Fourier analysis and scattering spectra results for L = 2.5 and 5μm. We excite the even propagating surface plasmon mode with a horizontally oriented dipole source. As can be seen, for a finite particle length, this mode is nothing more than the superposition of many higher order modes.

A. Farhang, Optics Express vol. 19, p. 11387 (2011)

SPP tunneling

- Long-range SPP can tunnel over large interruptions

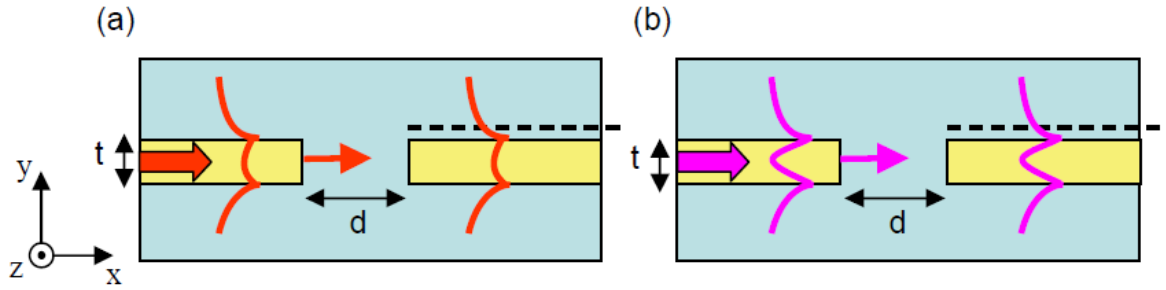

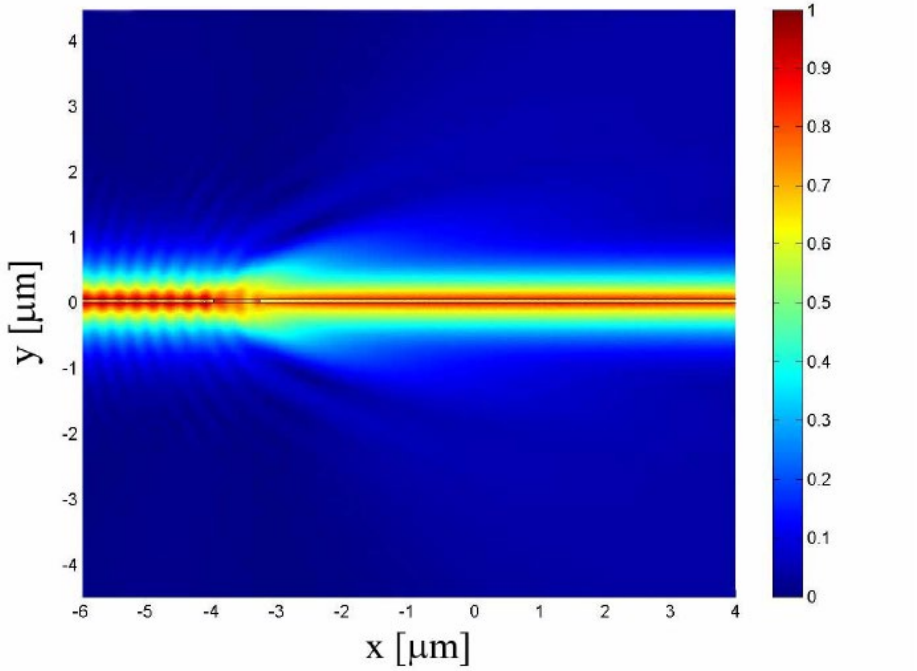

Fig. 8. Amplitude of magnetic field when a LR SPP mode is propagating on a t=40 nm thick gold film with a d=700 nm interruption, see Fig. 7(a). The movie shows the field distribution for interruptions between d=50 nm and d=4.7 μm.

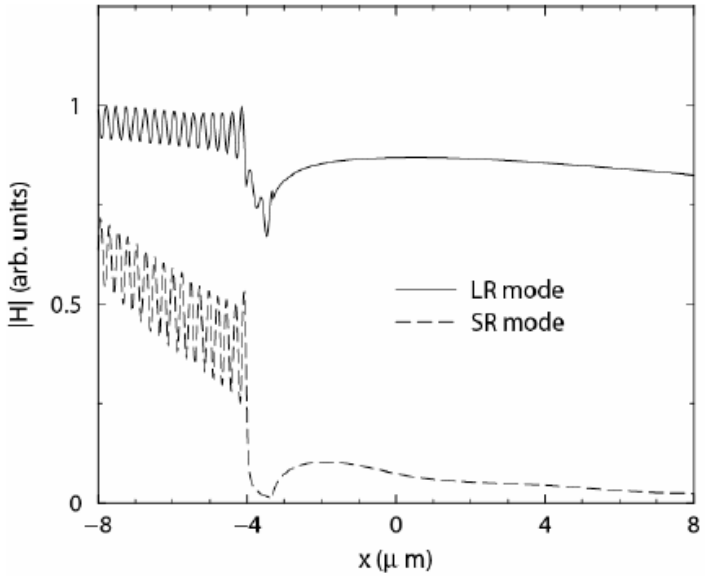

Fig. 9. Amplitude of the magnetic field 5 nm above the t=40 nm thick metallic film (see the dashed lines in Fig. 7) for long-range (LR) and short-range (SR) excitations. The film has a d=700 nm long interruption.

S. Sidorenko, Optics Express vol. 15, p. 6380 (2007)

Selected Topics in Advanced Optics

Week 6 – part 4

Olivier J.F. Martin
Nanophotonics and Metrology Laboratory

EPFL

Plasmonic waveguides

- Strip:

- Dielectric loaded:

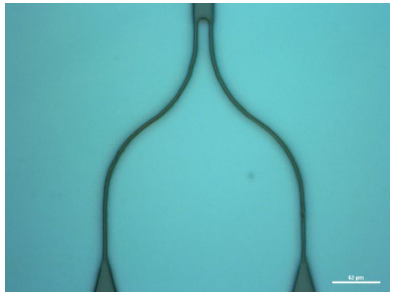

- Groove or channel:

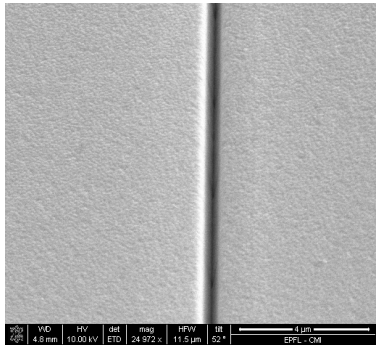

Asymmetric plasmonic strip waveguide

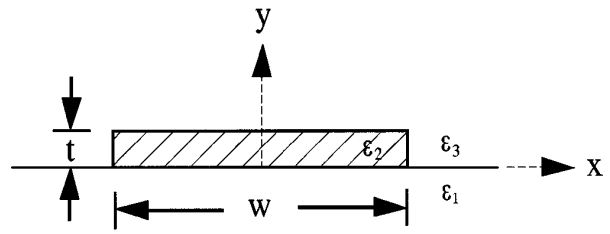

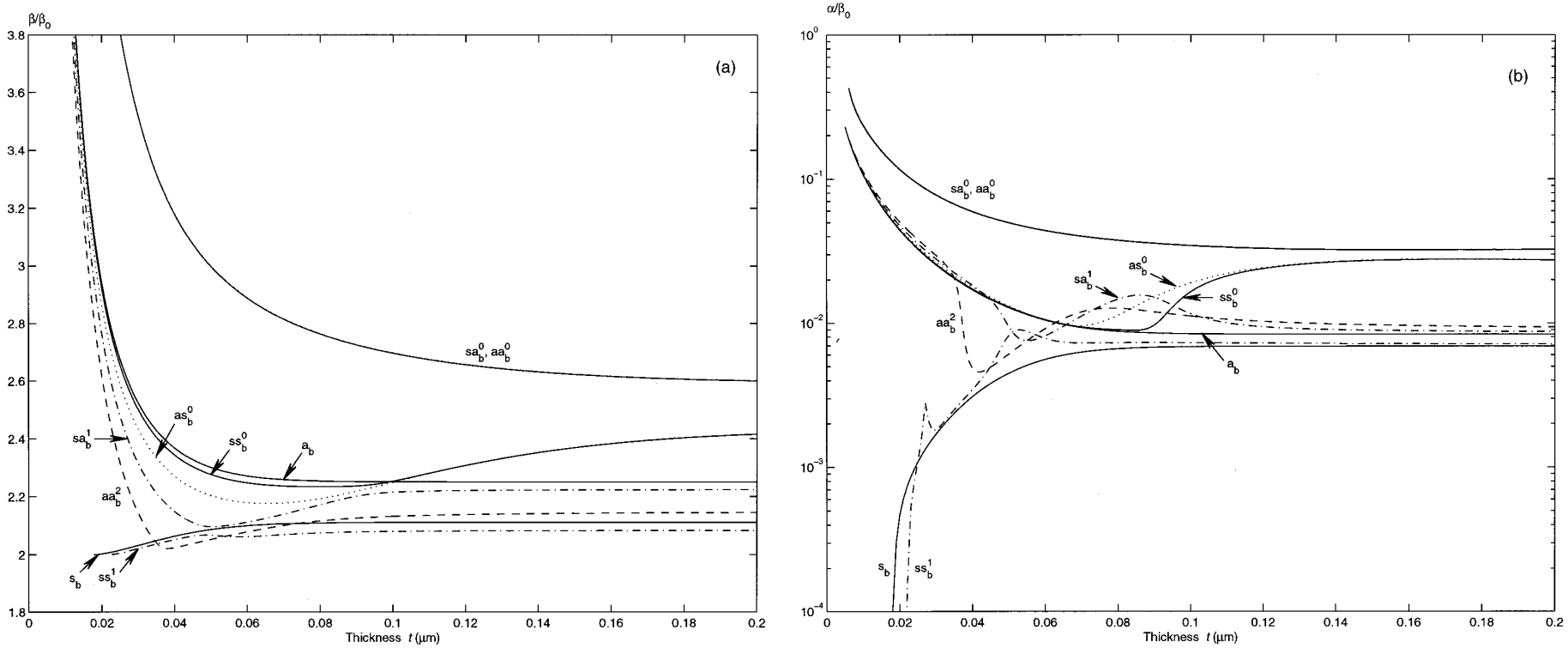

P. Berini et al., “Plasmon-polariton waves guided by thin lossy metal films of finite width: Bound modes of asymmetric structures”, *Phys. Rev. B*, vol. 63, p. 125417 (2001).

Symmetric plasmonic strip waveguide

Poynting vector

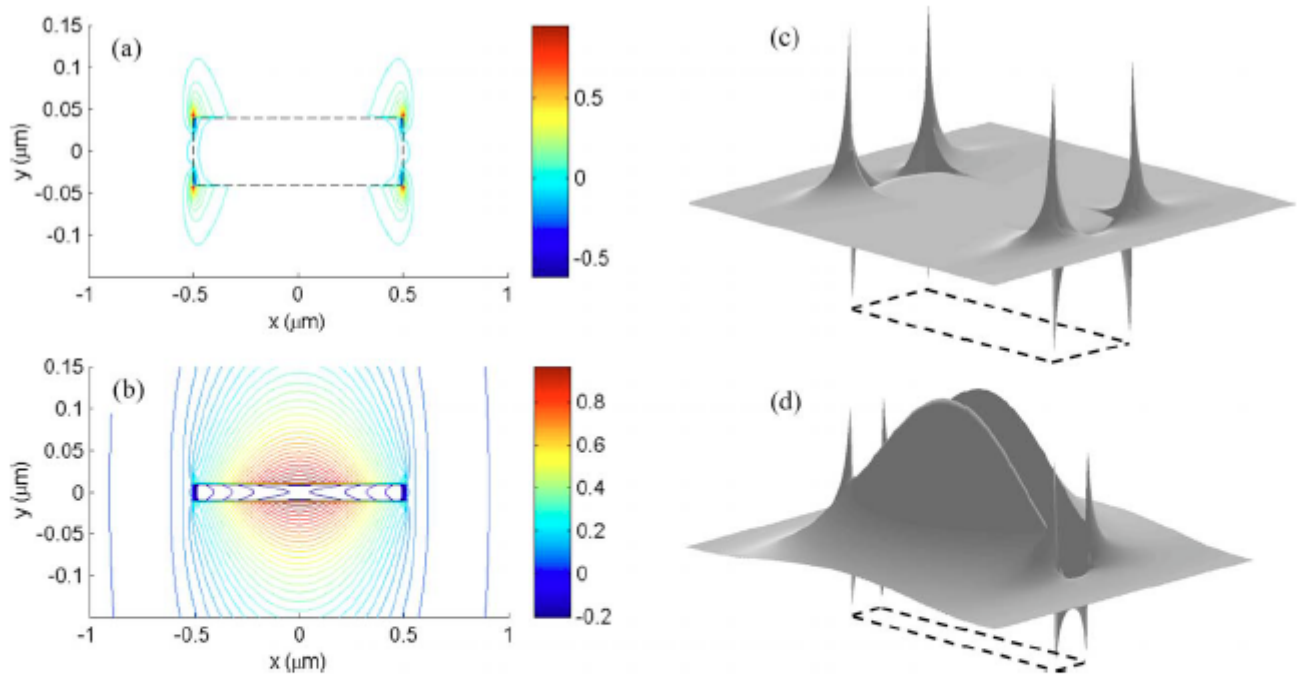

Contour and 3D plots of Re$\{S_z\}$ of the $ss_b{}^0$ mode for $w=1$ μm. (a) $t=80$ nm, (b) $t=20$ nm, (c) $t=100$ nm, (d) $t=40$ nm. All other parameters are the same as in Fig. 17 ($\lambda_0=633$ nm, $\varepsilon_{r,2}=-19-j0.53$ and $\varepsilon_{r,1}=\varepsilon_{r,3}=4$). The outline of the metal film is shown as the rectangular dashed contour. Adapted from Fig. 2 of [246], © 1999 Optical Society of America, and Fig. 7 of [248], © 2000 American Physical Society.

P. Berini et al., "Plasmon-polariton waves guided by thin lossy metal films of finite width: Bound modes of asymmetric structures", *Phys. Rev. B*, vol. 63, p. 125417 (2001).

Characterization of long-range strip waveguides

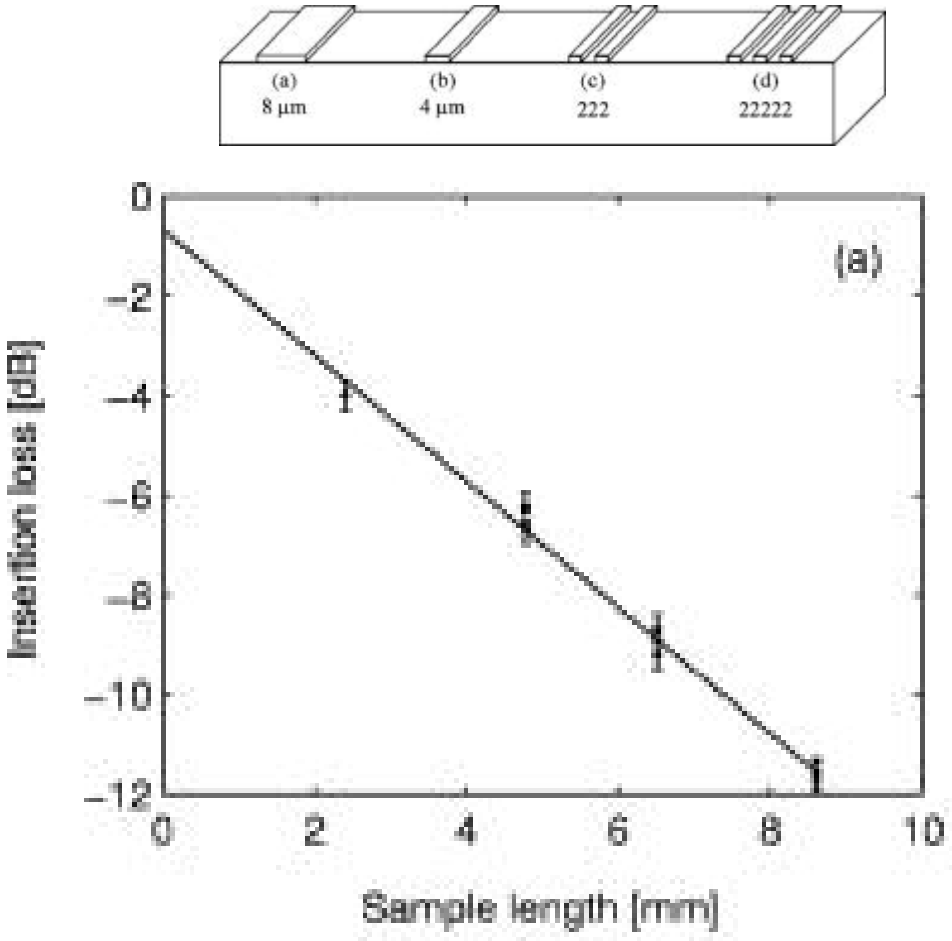

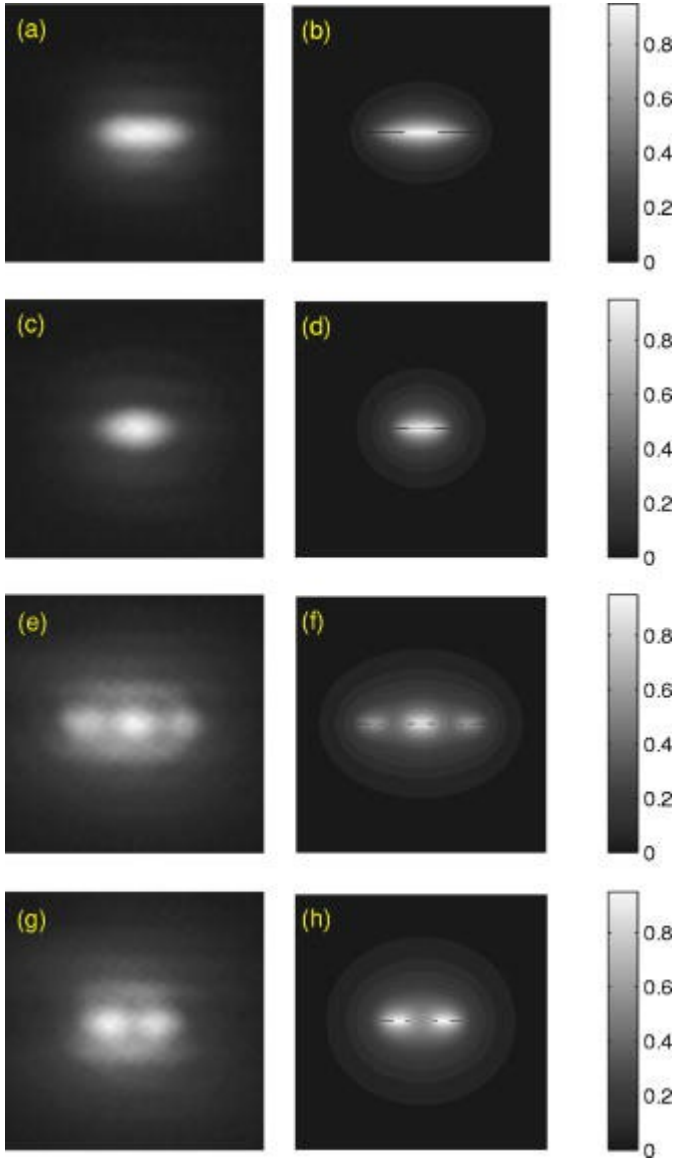

P. Berini et al., “Characterization of long-range surface-plasmon-polariton waveguides”, *Journal of Applied Physics*, vol. 98, p. 43109 (2005).

Dielectric loaded plasmon waveguide

- The dielectric load confines the plasmon that propagates on the metal film
- The more field in the metal, the better light confinement but the shorter propagation distance

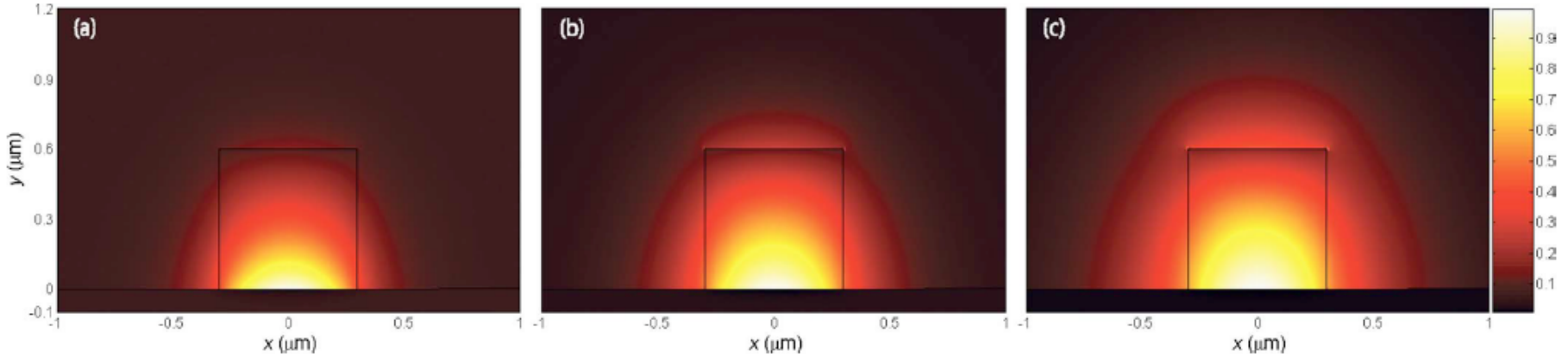

FIG. 7. (Color online) Field distribution plots of the magnitude of the vertical component of the electric field $|E_y|$ for ridge dimension t=600 nm, w=600 nm, calculated by application of the FEM. In all three plots, the fundamental TM_{00} mode is depicted. (a) shows the field for λ=893 nm (n_3=0.21+i5.94) where N_{eff}=1.49 and L=16.1 μm, (b) for λ=1.22 μm (n_3=0.36+i8.60) where N_{eff}=1.39 and L=29.8 μm, and (c) for λ=1.55 μm (n_3=0.55+i11.5) where N_{eff}=1.29 and L=44.4 μm (Ref. 28).

T. Tobias Holmgaard et al., "Theoretical analysis of dielectric-loaded surface plasmon-polariton waveguides," *Phys. Rev. B* **75**, 245405 (2007).

Dielectric loaded plasmon waveguide

- Dielectric strip made of PMMA

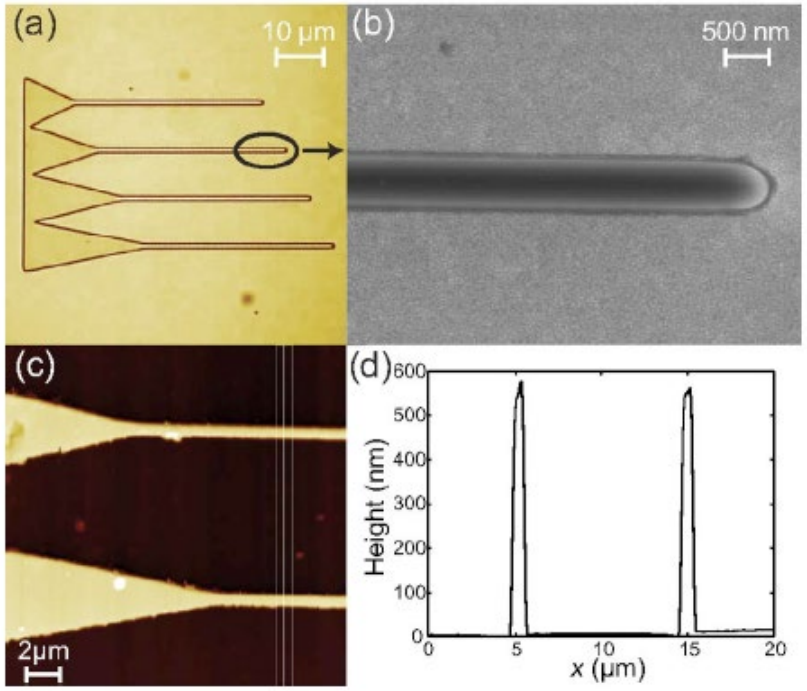

FIG. 1. (Color online) (a) Microscope image of a block with four waveguides with in coupling funnel of different dimensions. (b) SEM image of the termination region of a straight waveguide, revealing a waveguide width of ~500 nm. (c) AFM image of the tapering region and (d) cross section of the AFM image revealing a waveguide height of ~550 nm.

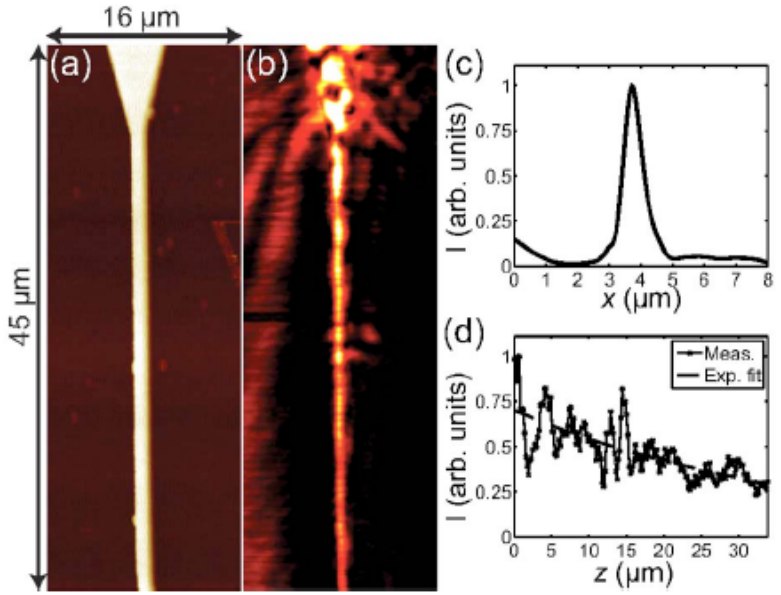

FIG. 3. (Color online) Near-field optical measurements of a straight DL-SPPW with a 10×25 μm in coupling funnel. [(a) and (b)] Topographical and near-field optical signal images, respectively, for $\lambda = 1550$ nm. (c) Cross section of the optical image perpendicular to the waveguide and (d) averaged profile of the near-field optical signal recorded along the waveguide.

T. Tobias Holmgaard et al., "Dielectric-loaded surface plasmon-polariton waveguides at telecommunication wavelengths: Excitation and characterization," *Appl. Phys. Lett.* **92**, 011124 (2008).

FIB fabrication for groove (channel) waveguides

- FEI Nova 600 Nanolab dual-beam (FIB/SEM)

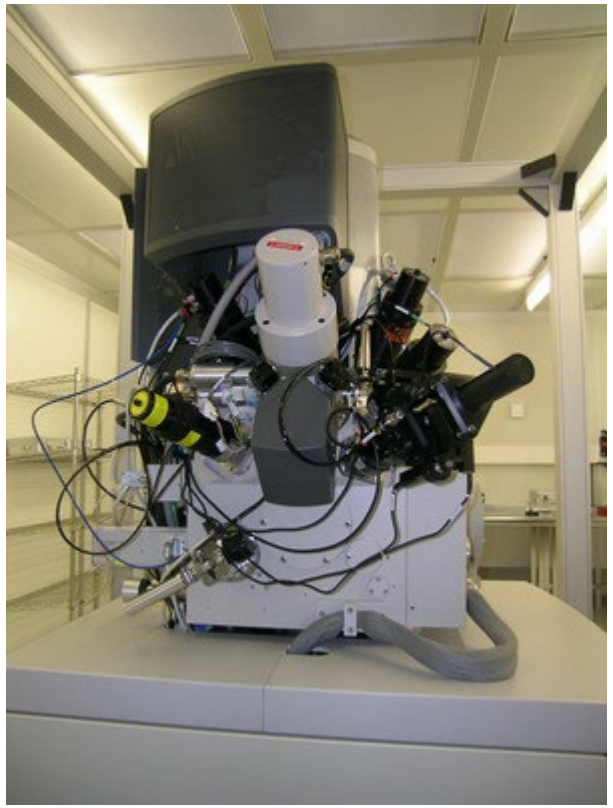

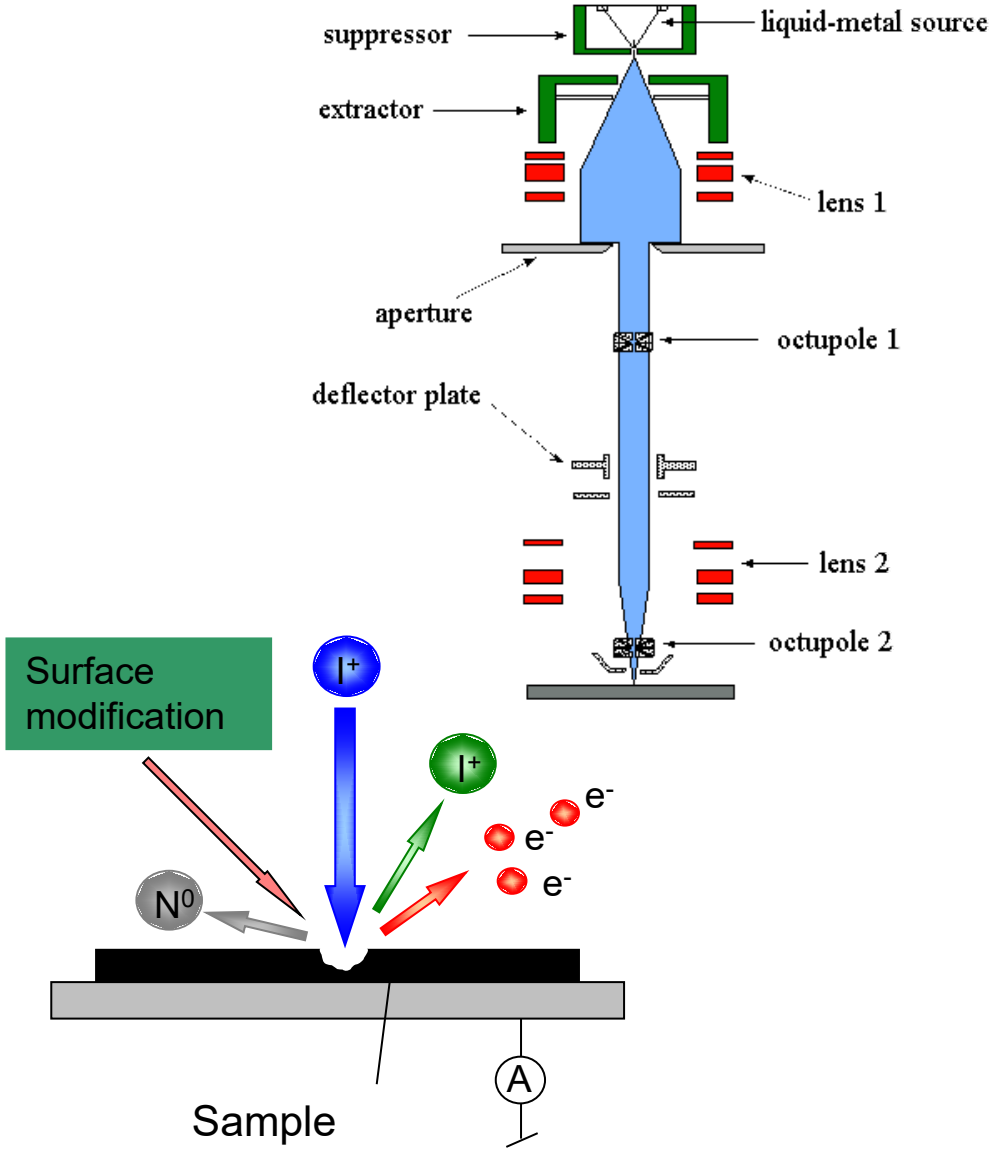

FIB fabrication for groove (channel) waveguides

- Only relatively narrow grooves can be milled easily…

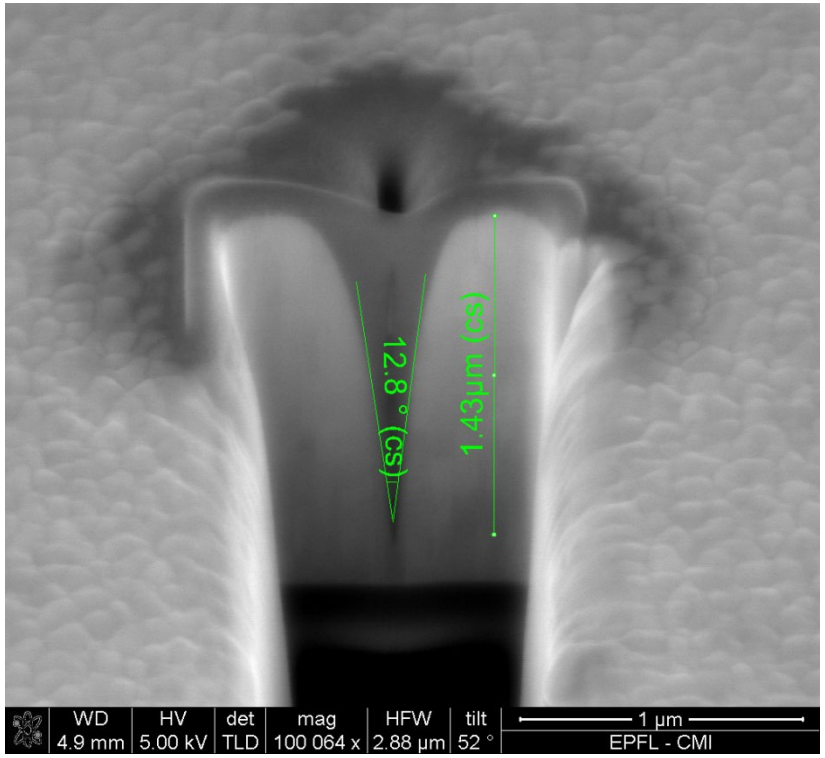

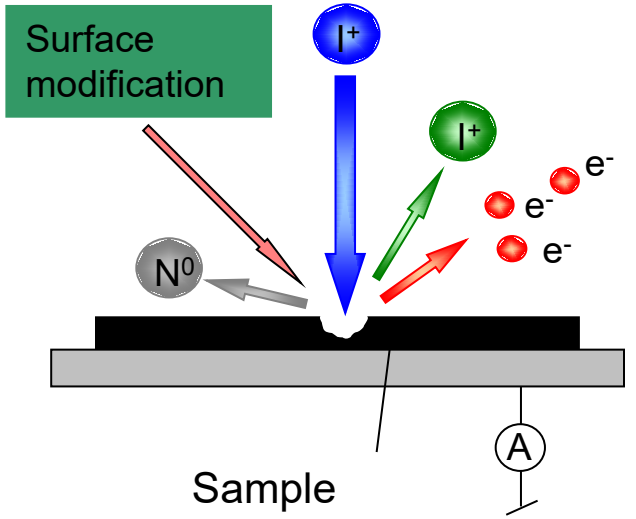

Plasmonic modes of groove/wedge waveguides

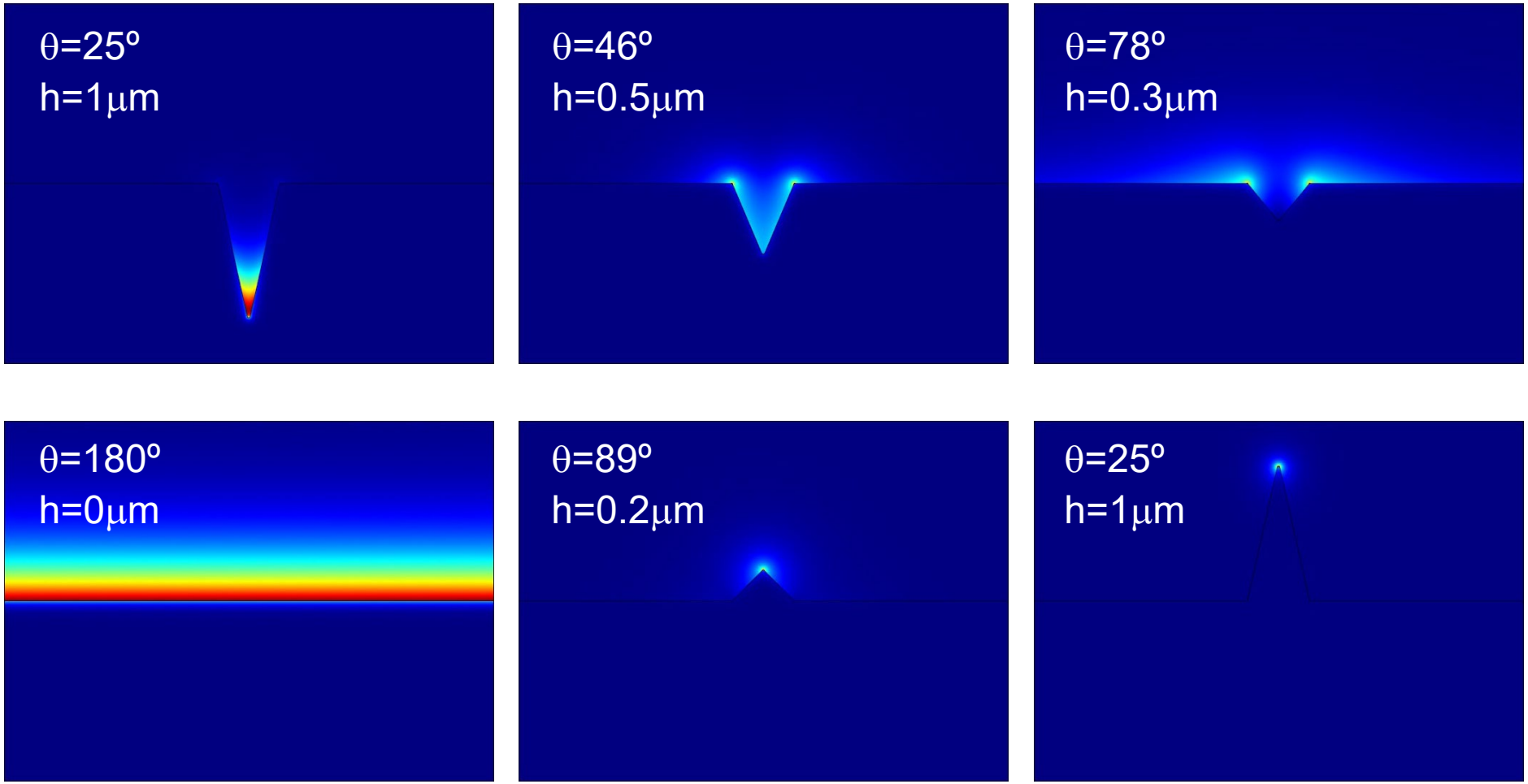

• Au film, λ=1.55μm

J. Dintinger, Optics Express vol. 17, p. 2364 (2009)

Groove/wedge waveguides

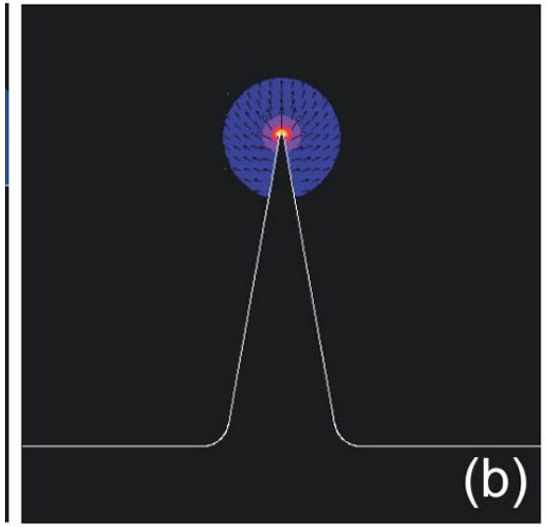

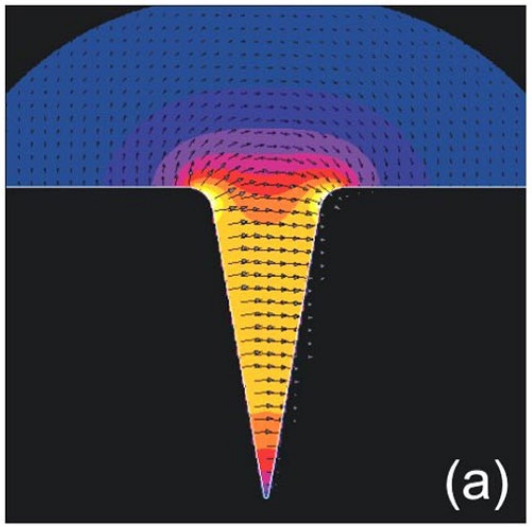

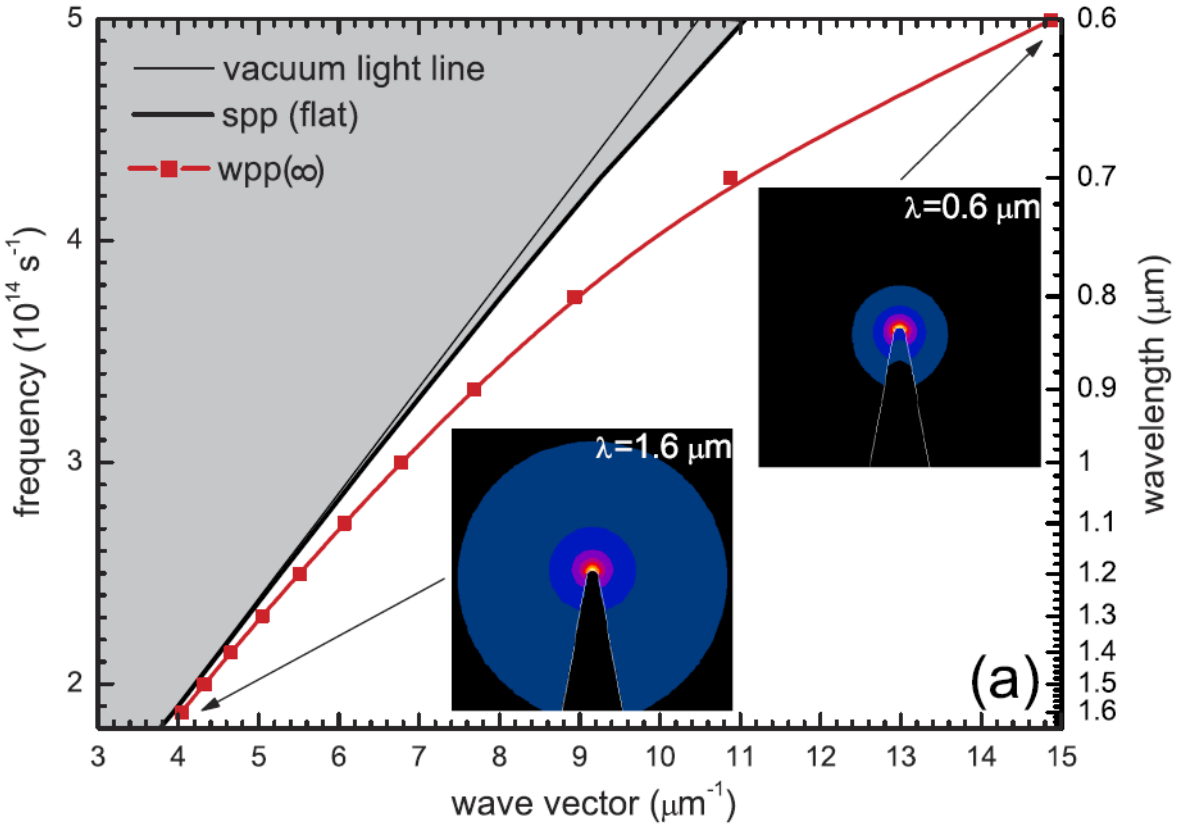

E. Moreno et al., “Guiding and Focusing of Electromagnetic Fields withWedge Plasmon Polaritons”, *Physical Review Letters* vol. 100, p. 023901 (2008).

Groove (channel) waveguides

Y-splitter

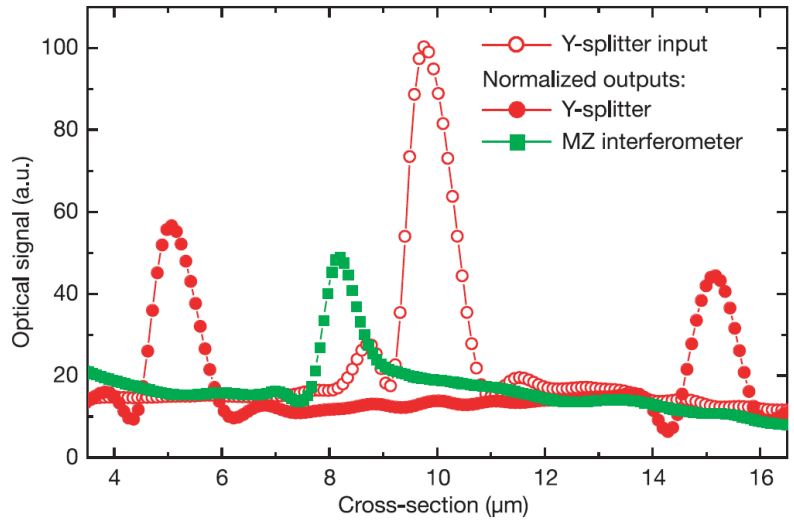

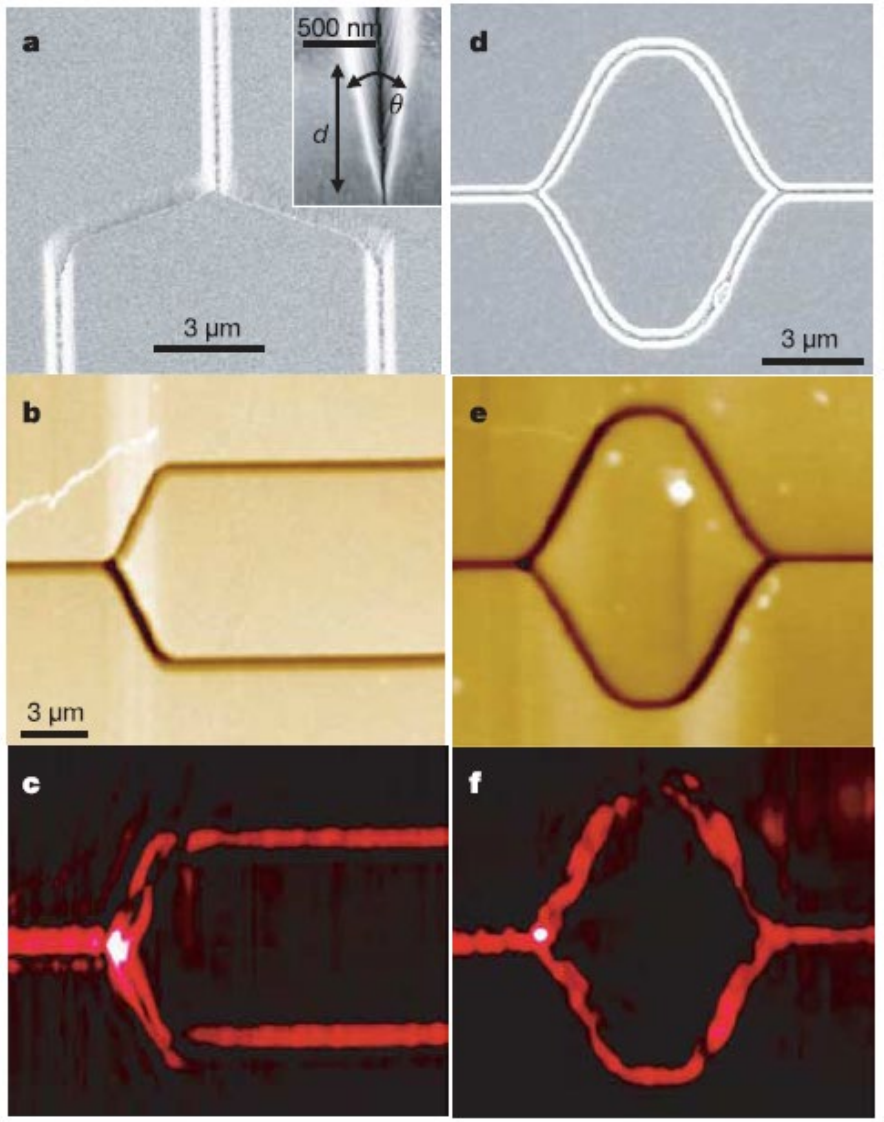

Mach-Zhender interferometer

S.I. Bozhevolnyi, “Channel plasmon subwavelength waveguide components including interferometers and ring resonators”, Nature vol. 440, p. 508 (2006).

Groove (channel) waveguides

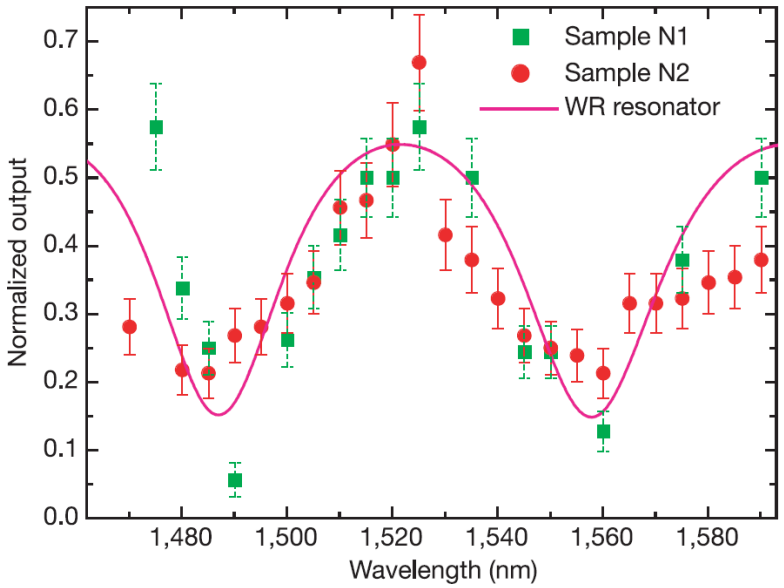

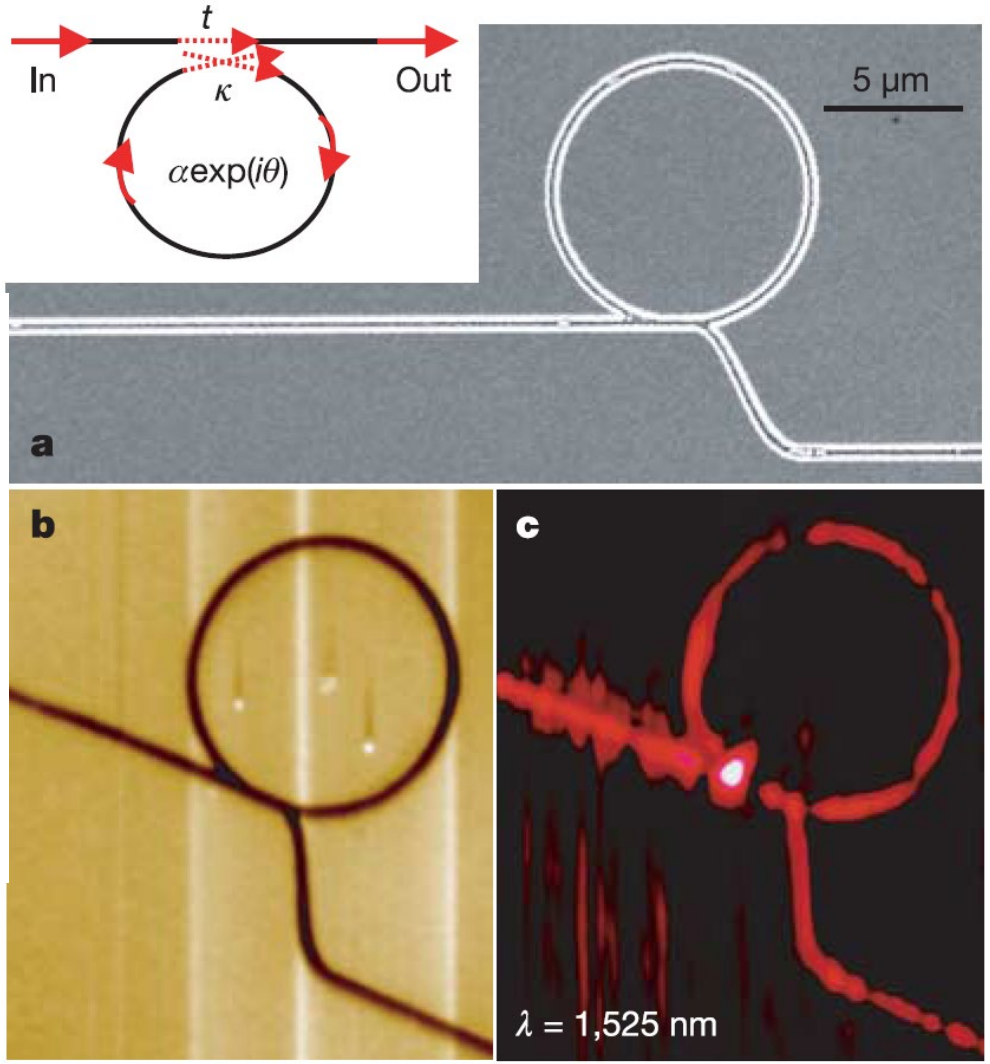

Ring resonator

S.I. Bozhevolnyi, “Channel plasmon subwavelength waveguide components including interferometers and ring resonators”, Nature vol. 440, p. 508 (2006).

Single crystal plasmonic flakes

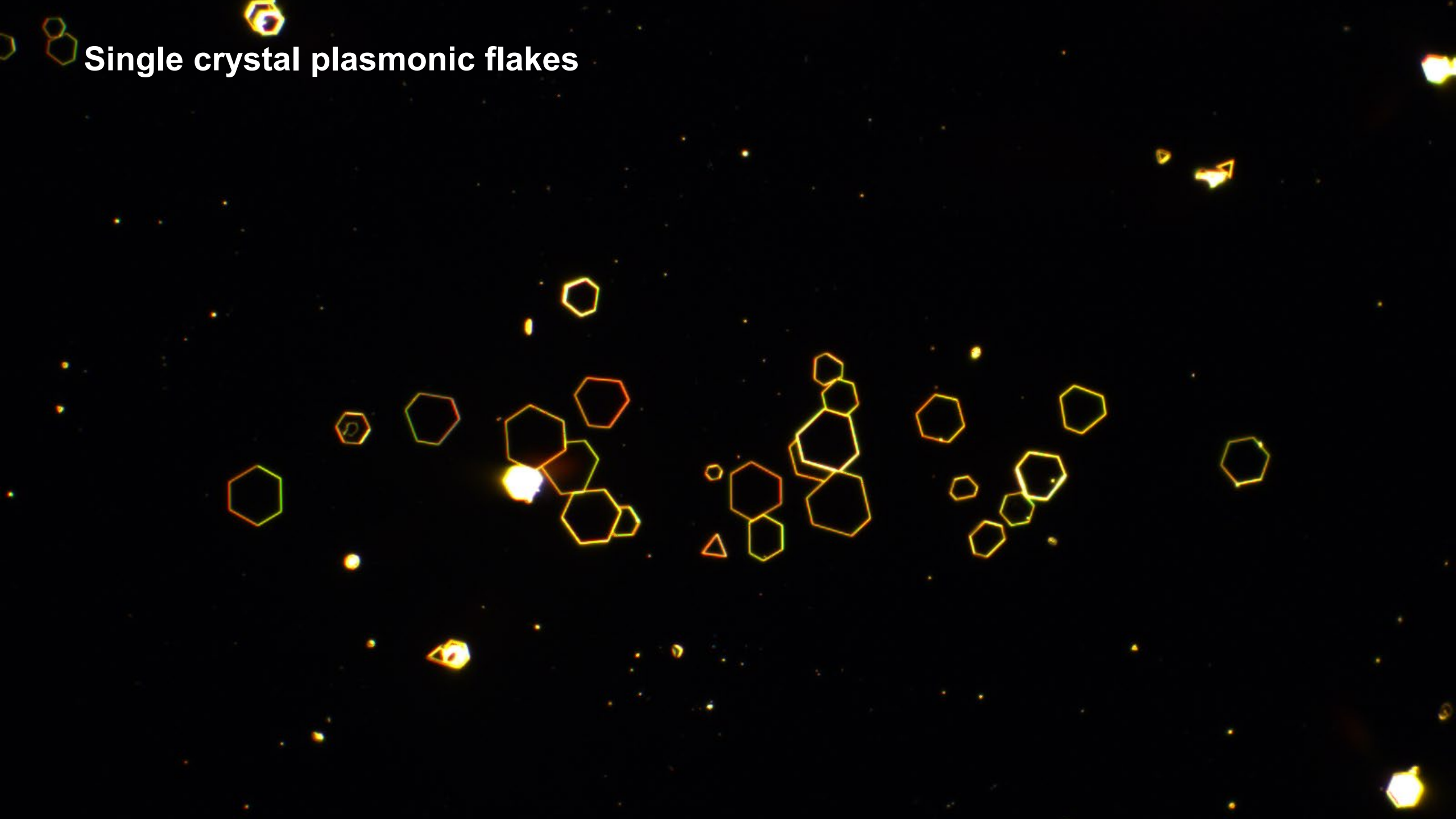

Growing monocrystalline gold and silver flakes

1. Mix ethylene glycol with chloroauric acid $HAuCl_4$

2. Grow on Si or SiO2 substrate overnight at 70-80 °C

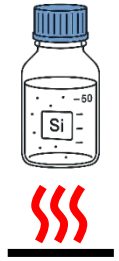

- Add ammonia (NH_4OH) into Ethylene glycol

- Add silver nitrate salt ($AgNO_3$)
- Add polyvinylpyrrolidone (PVP)
- Add chloroplatinic acid hydrate ($H_2PtCl_6 \cdot xH_2O$)

- Add hydrogen peroxide (H_2O_2)

- Grow on Si or SiO_2 substrate for 3-7 days at room temperature

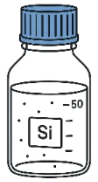

E. Krauss, Crystal Growth & Design vol. 18, p. 1297 (2018)
C.-Y. Wang, Nature Communications vol. 6, p. 7734 (2015)

Single crystal gold flakes

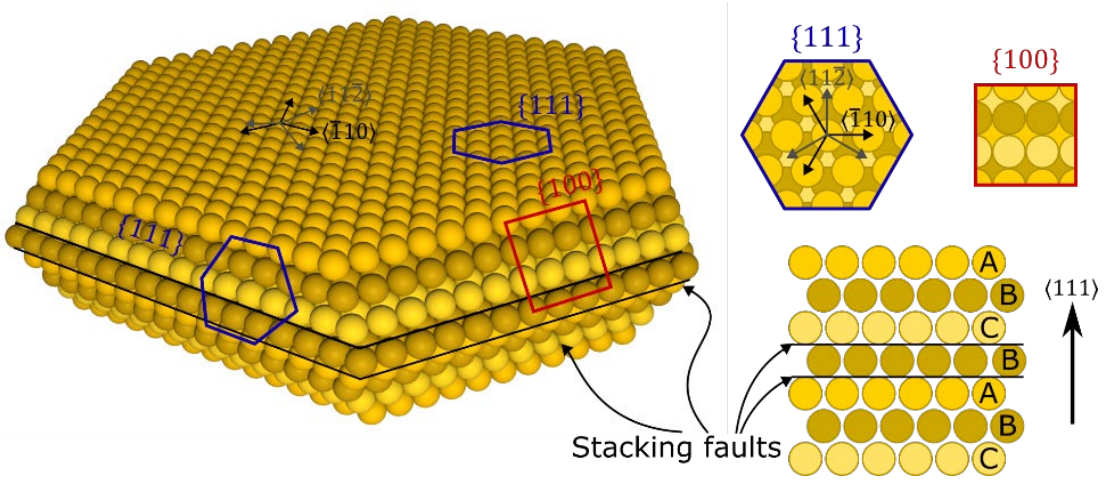

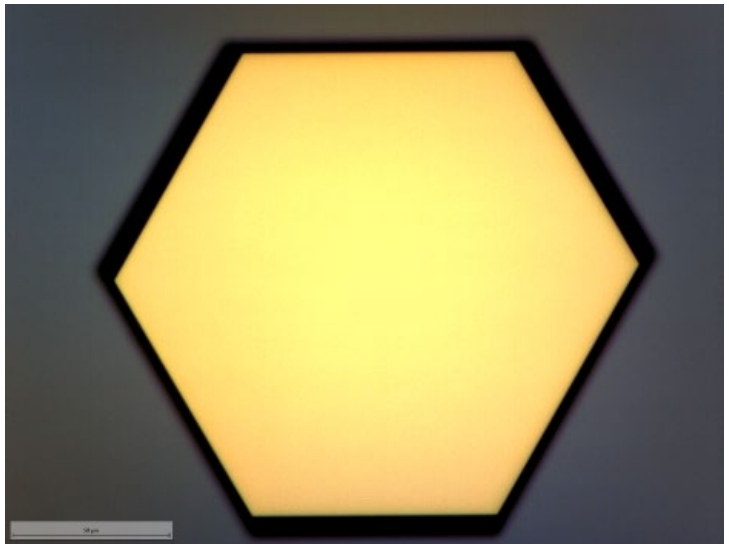

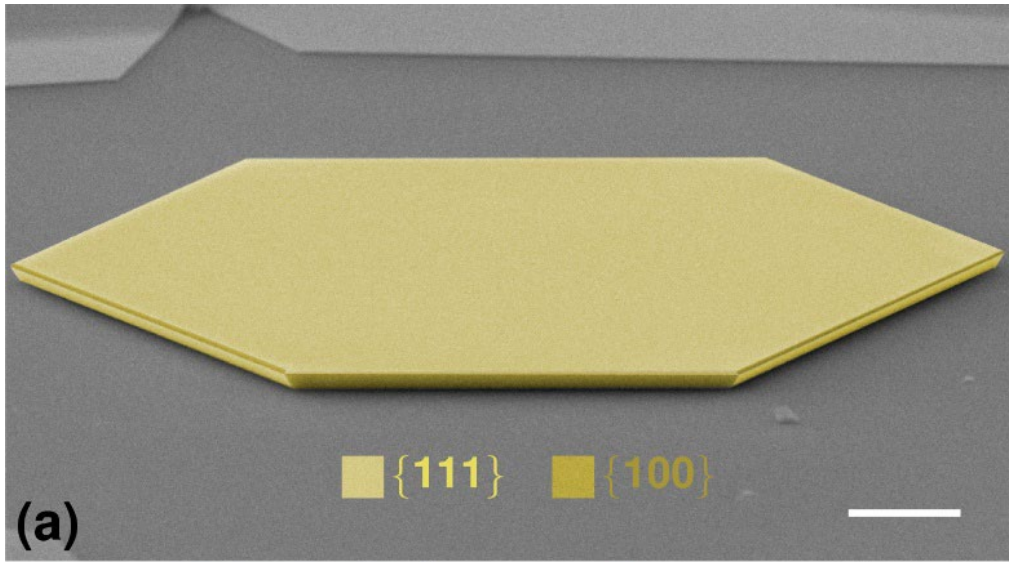

Opt. Mater. Express 8, 3688 (2018)

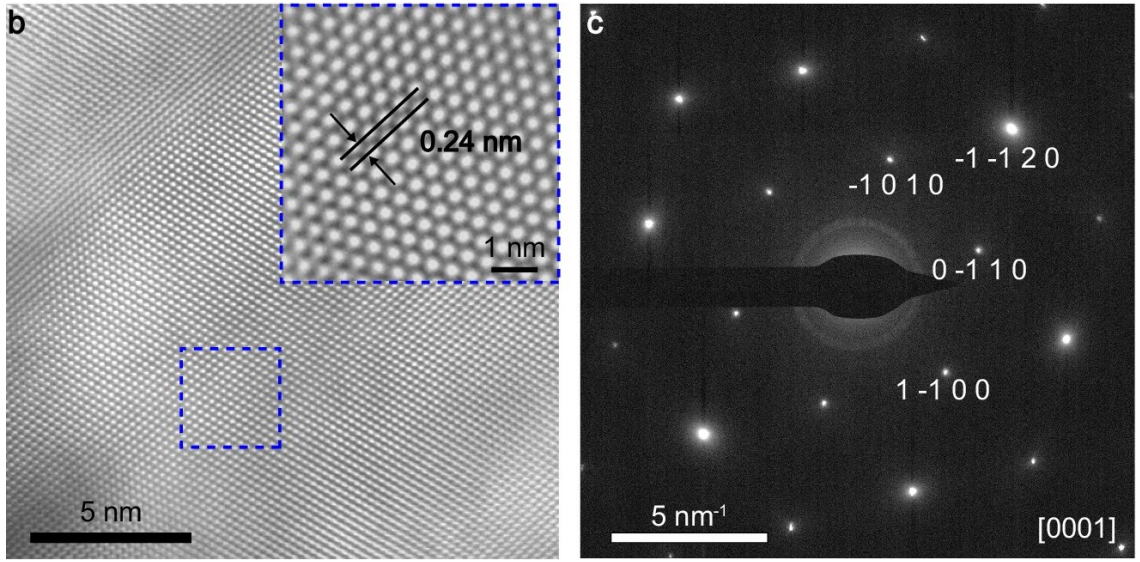

Nat. Commun. 15, 2840 (2024)

Single crystal gold flakes

- Can be structured using Focused Ion Beam
- Provide very smooth surfaces

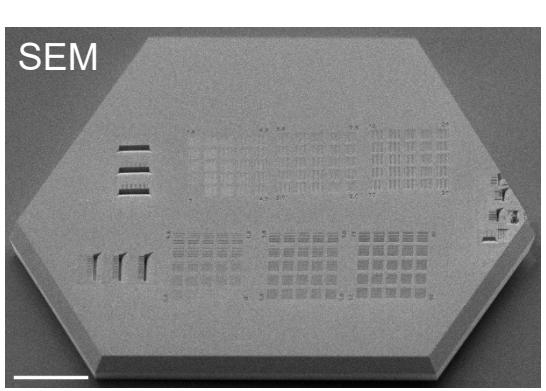

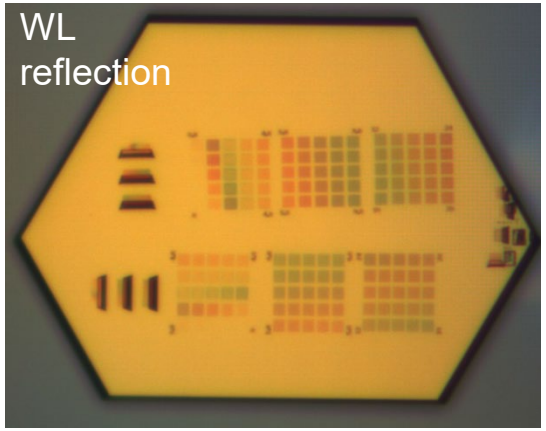

0.2 pC/µm

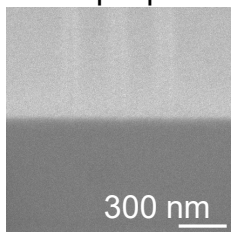

5 pC/µm

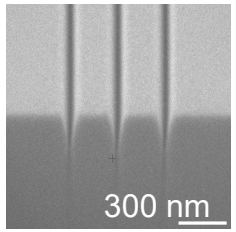

10 pC/µm

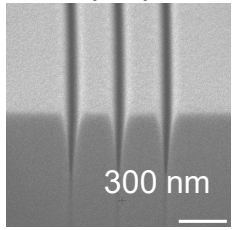

{111} surface
along $\langle \bar{1}10 \rangle$ axis

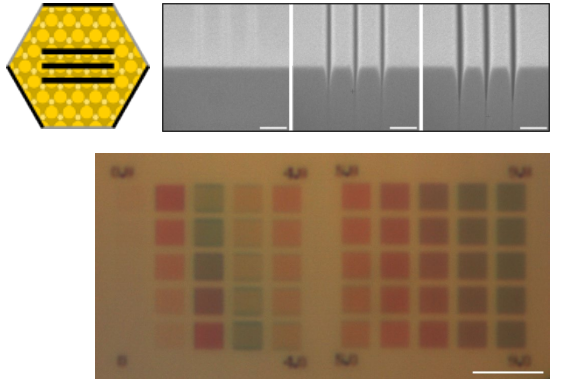

{111} surface
along $\langle 11\bar{2} \rangle$ axis

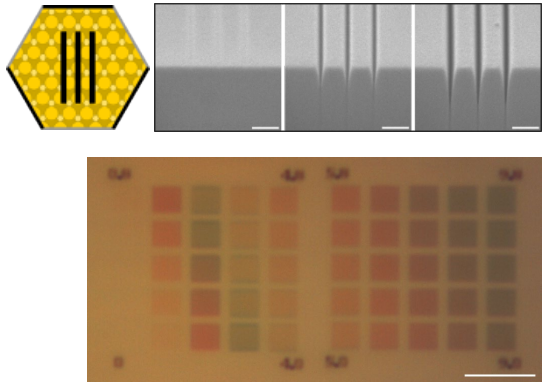

Polycrystalline surface

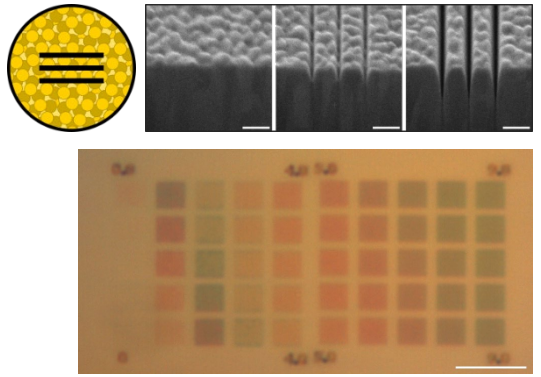

Single crystal gold flakes

- Provide access to the crystalline nature → anisotropic properties,
  e.g. for the nonlinear response of gold